TRANSPORTATION RESEARCH RECORD

584

Pavement Surface Properties and Vehicle Interaction

5 reports prepared for the 54th Annual Meeting of the Transportation Research Board

TRB

TRANSPORTATION RESEARCH BOARD

NATIONAL RESEARCH COUNCIL

Washington, D. C., 1976

Transportation Research Record 584
Price $2.80
Edited for TRB by Joan B. Silberman

Subject areas
26 pavement performance
51 highway safety

The project that is the subject of this report was approved by the Governing Board of the National Research Council, whose members are drawn from the councils of the National Academy of Sciences, the National Academy of Engineering, and the Institute of Medicine. The members of the committee responsible for the report were chosen for their special competence and with regard for appropriate balance.

This report has been reviewed by a group other than the authors according to procedures approved by a Report Review Committee consisting of members of the National Academy of Sciences, the National Academy of Engineering, and the Institute of Medicine.

LIBRARY OF CONGRESS CATALOGING IN PUBLICATION DATA

National Research Council. Transportation Research Board.
Pavement surface properties and vehicle interaction.

(Transportation research record; 584)

1. Pavements–Design and construction–Addresses, essays, lectures. 2. Pavements–Testing–Addresses, essays, lectures. 3. Motor vehicles–Skidding–Addresses, essays, lectures. 4. Roads–Riding qualities–Testing–Addresses, essays, lectures. I. Title. II. Series.
TE7.H5 no. 584 [TE251] 380.5'08s [625.8'028] 76-40976
ISBN 0-309-02498-6

CONTENTS

FOREWORD

Recently there have been continuing efforts to determine how best to use methods to ensure the production of long-lasting pavement surfaces possessing satisfactory wet skid-resistant characteristics. Considerable work has also been conducted on road roughness with regard to both highway safety and rider comfort. The papers in this Transportation Research Record describe the results of work on both road roughness and skid resistance and should be of particular interest to highway material, design, and research engineers.

Dahir, Meyer, and Hegmon report the results of an extensive cooperative effort between industry and the Pennsylvania Department of Transportation to evaluate bituminous pavements and aggregate polishing. Their studies were designed to determine whether practical correlations exist between field skid results and various laboratory measurement and polishing techniques. Environmental, traffic, and petrographic characteristics of surface aggregates were found to influence pavement field performance to some degree; however, general trends only, rather than specific relationships, were predictable.

Dunlap, Fancher, Jr., Scott, MacAdam, and Segel develop a mathematical equation that expresses the required skid number for safe operation of a vehicle on a pavement surface, given certain roadway design characteristics. The characteristics of concern included variations in vehicles, tires, road surfaces, curvature, super elevation, grade, and specific maneuvers.

Rizenbergs, Burchett, Deacon, and Napier took friction measurements with a skid trailer at 70 mph (31 m/s) on 777 miles (1240 km) of rural, four-lane, controlled-access Interstate and parkway routes throughout Kentucky. The expression of accident occurrence found to correlate best with skid and slip resistance was wet-weather accidents per 100 million vehicle miles (161 million vehicle km). As the skid numbers at 70 mph (31 m/s) decreased from 27, accident frequency increased greatly. Peak slip numbers and accident occurrence displayed similar trends.

Williamson describes the use of digital filters to analyze road profiles measured by a profilometer. The purpose of filtering the signals was to isolate roughness of a given type for future analysis. Test cases were used to compare and demonstrate the capabilities of selected filters. A particular recursive filter, designed by the tangent form of the squared-magnitude approximating function, is recommended for use in analyzing road profiles.

Park and Wambold describe the research to establish a correlation between objective and subjective comfort ratings of vehicles (i.e., buses) traversing rough roads. A correlation of absorbed power (a function of energy flow and the anatomical properties of the human body), an objective ride measure, to the subjective evaluation of ride comfort by individuals was developed.

—F. A. Renninger

LABORATORY AND FIELD INVESTIGATION OF BITUMINOUS PAVEMENT AND AGGREGATE POLISHING

S. H. Dahir, Department of Civil Engineering, Pennsylvania State University, Middletown;
W. E. Meyer, Department of Mechanical Engineering, Pennsylvania State University, University Park; and
R. R. Hegmon, Office of Research, Federal Highway Administration

To investigate the field performance of aggregates, 11 test strips containing replicate sections of bituminous pavements used in Pennsylvania were designed and constructed by a joint industry-Pennsylvania Department of Transportation task force. In the investigation, 52 aggregate samples and 223 pavement cores of the test sections were polished in the laboratory by using various polishing methods and friction measurement techniques. Correlations between field and laboratory data were sought, and factors associated with skid-resistance variations were observed and investigated. Laboratory-field data correlations indicated that the general level of skid-resistance characteristics of surface aggregates may be determined in the laboratory and that the aggregates may be ranked similarly by both approaches. However, the correlations failed to produce regression equations that could, with confidence, define specific mathematical relationships for predicting specific field skid numbers. A minimum field skid number occurred in the late summer and fall and correlated better with laboratory results than a mean skid number. The minimum number appears to stabilize after 2 years of pavement exposure to traffic, irrespective of the level of traffic. Higher average daily traffic produced a lower skid-resistance level, and one truck was equivalent to about 18 passenger cars in polishing effects. Cumulative traffic also caused reduction in the skid number until the surface stabilized; then the number leveled off. Temperature correction of the minimum skid number appears to have little or no effect on skid data analysis. Increase in the percentage of insoluble residue of carbonate aggregates indicated only possible increases in skid resistance, but no dependable quantitative correlation could be obtained from available tests.

•RECENTLY, there has been a continuing effort in Pennsylvania to arrive at satisfactory, updated solutions to the problem of how best to use available materials and methods for providing long-lasting pavement surfaces with wet skid-resistance characteristics. As part of this effort, a cooperative laboratory-field skid-resistance testing program has been conducted in Pennsylvania since 1968, primarily to evaluate aggregate skid-resistance performance on bituminous surfaces. Eleven test strips (1) planned by Pennsylvania Department of Transportation and industry were constructed in 11 geographic locations of the state and have been monitored for field skid-resistance data. The Pennsylvania State University (Penn State) Automotive Research Program conducted part of the laboratory investigations on bituminous pavement polishing (8). Laboratory and field data were pooled and analyzed so that laboratory polishing performance of aggregates could be obtained for establishing correlations with field skid data from Pennsylvania DOT test strips and for determining the effects of aggregate type and other related factors on surface skid resistance.

Laboratory data were obtained by using three polishing methods, three friction measuring techniques, and four sample forms. Field data were obtained on the test strips periodically by Pennsylvania DOT by using skid trailers conforming to ASTM E 274 at

40 mph (64 km/h). Other pertinent data were also obtained and used in the analysis and discussion. All tests were performed on aggregates and sections used in the test strip program.

Results of laboratory tests using various procedures were correlated with one another and with field skid resistance. Other factors influencing skid resistance, such as time, traffic, and insoluble residue of carbonate aggregates, were also investigated when they were relevant to the research.

AGGREGATE POLISHING

Fifty-two samples from 10 aggregate types representing those used in the test strip program were supplied by Pennsylvania DOT. The strips included 156 replicate sections of 1,000-ft (304.8-m) length or more each, totaling about 44 lane miles (13.4 km). Test strip layouts and pertinent data have been documented in department reports (1, 2). A summary of the test strip sections and of the aggregates used in the polishing program is given in Table 1.

All aggregate samples were polished. From each sample, two 4 by 12-in. (102 by 305-mm) panels were prepared by setting ¼ to ⅜-in. (6.35 to 9.53-mm) aggregate particles in an epoxy matrix. The panels were polished with the Penn State rotary drum polishing machine (RDM) (3). Panel frictional resistance was measured with the Penn State drag tester (3) in drag tester numbers (DTN) and with the British portable tester (BPT) in British portable numbers (BPN), according to ASTM E 303-69. An overall view of the rotary drum machine (RDM) is shown in Figure 1.

In addition, two other 3 by 5-in. (76 by 127-mm) panels were similarly prepared and polished with the modified Penn State reciprocating pavement polisher (RPP) (3), and frictional resistance was measured with the British portable tester in BPN units. An overall view of the RPP is shown in Figure 2.

Two other simplified aggregate polishing methods were investigated: the jar mill tumbler used in North Carolina (4) and a small drum machine (SDM) used for aggregate wear at Penn State (5) and modified for use in this project.

In the case of the jar mill tumbler, polishing of loose, coarse individual aggregate particles was easy to achieve, but there was no convenient way to measure the frictional properties of the aggregate particles. The particles had to be molded into a Plaster of Paris cast, then the average friction was measured with the British portable tester. This procedure seemed to defeat the objective of a simplified approach. For this reason, the jar mill tumbler method was not pursued beyond the trial stage.

As an alternate simplified procedure, the SDM was modified to polish up to 10 individual ¼-in. (6.35-mm) particles of the same aggregate and, simultaneously, to measure the average frictional resistance of the particles electronically. A general view of the modified SDM and friction-measuring equipment is shown in Figures 3 and 4.

Experience with aggregate polishing has shown that carbonate aggregates generally polish more evenly than most other aggregate types. For this reason, samples prepared from 15 available limestones were polished and tested for frictional resistance by using the SDM and other methods. In addition, 223 pavement cores representative of the test sections and supplied by Pennsylvania DOT under a different, but related, project (6) were also polished with the RPP, and friction was measured by using the BPT. A summary of the laboratory polishing results obtained by the various methods on the tested aggregate and core samples is given in Table 2. Also included in Table 2 is a summary of field testing data that will be discussed later.

COMPARISON AND CORRELATION OF LABORATORY TEST RESULTS

Comparison of the laboratory-polishing and friction-measurement procedures was achieved by plotting results obtained on the 15 limestone aggregates polished and tested by all the methods used in the research. These results (given in Table 2) are shown in

Table 1. Test strip sections and aggregate samples tested for polishing.

Aggregate Type	Number of Sources	Number of Test Sections	Length (miles)	Number of Samples
Carbonates	20	59	25.43	
Limestone				15
Dolomite				4
Slags	8	20	3.73	9[a]
Gravels	9	18	3.83	9
Blends	15	29	5.27	—
Miscellaneous	12	30	5.62	
Argillite				7
Diabase				3
Quartzite				1
Gneiss				1
Sandstone				2
Siltstone				1
Total	64	156	43.88	52

Note: 1 mile = 1.6 km.
[a]Slag samples BO and BB were obtained from the same source.

Figure 1. Penn State rotary drum machine.

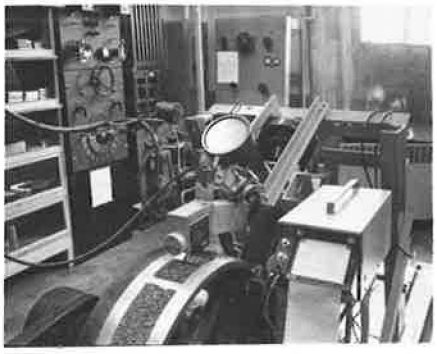

Figure 2. Penn State reciprocating pavement polisher.

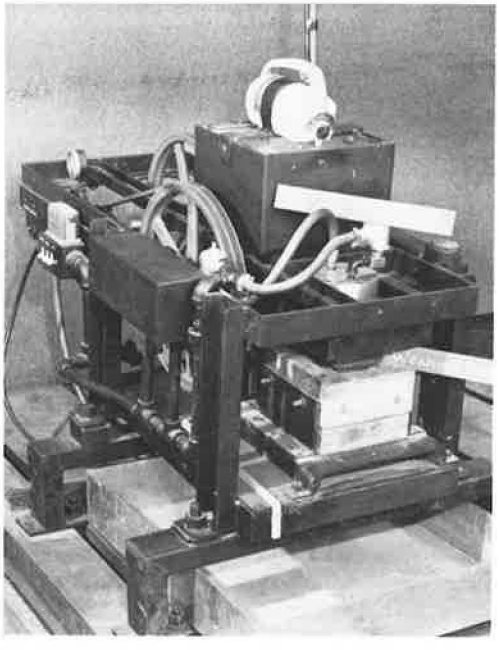

Figure 3. Modified small drum machine.

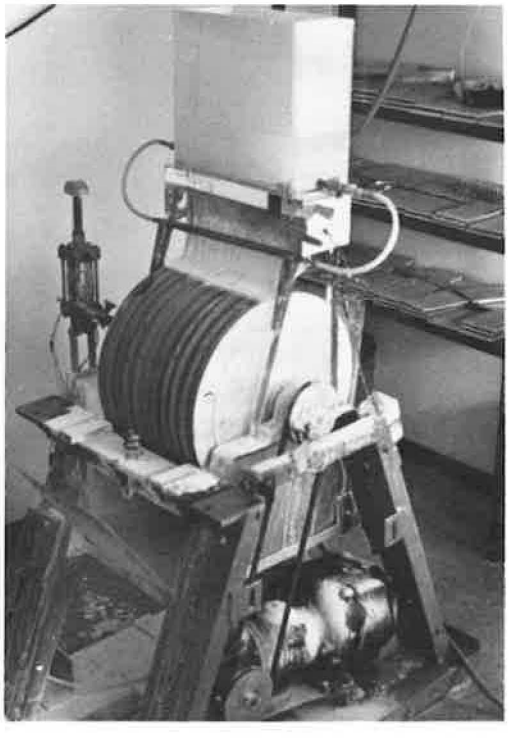

Figure 4. Aggregate particle mount.

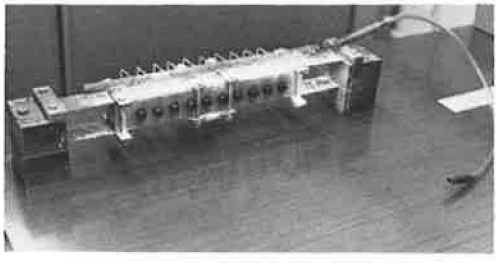

Table 2. Results of aggregate and pavement polishing and friction measurement by various procedures.

Aggregate	Percentage of Insoluble Residue	Laboratory Identification Number	Test Sections	SDM (f × 100)	4 by 12-In. Panel		3 by 5-In. Core		Minimum 3-Year Average	Minimum SN_{40}
					RDM DTN	BPT BPN	RPP	BPT BPN		
Limestone	6.3	44	2-1, 2-3, 2-8	34	33	31	60	50	41	36
	2.8	46	5-1	39	32	40	56	57	42	41
	24.1	47	5-4	41	32	40	69	63	46	44
	8.7	48	8-3	27	32	37	64	52	44	42
	37.5	49[a]	8-1	60	37	49	73	75	54	47
	1.0	50	9-6	24	29	33	53	55	41	35
	3.7	51	9-1	26	29	31	56	59	38	35
	37.5	52[a]	10-1	59	42	54	74	65	38	38
	38.4	53[a]	10-4	56	44	50	74	67	36	34
	1.2	55	11-1	32	42	37	67	64	46	41
	10.1	56	3-1	—	31	38	53	47	30	27
	1.5	57	3-2	24	31	33	54	48	27	21
	2.1	58	4-4	29	32	41	54	66	42	38
	0.8	59	6-1	27	32	39	58	43	33	25
	7.1	60	7-5	37	31	41	57	58	44	34
Avg				36.8	33.9	39.6	61.4	57	40	35
Dolomite	2.6	54	11-2	—	31	38	61	64	46	41
	2.2	61	7-1	—	32	37	55	59	48	37
	2.2	62	7-2	—	31	36	54	62	48	36
	0.9	91	1-2, 1-3, 1-4, 1-12, 1-25	37	32	41	—	48	44	38
Avg				37	32	38	57	53	45	38
Gravel[b]		70	1-13		65	62	73	65	51	45
		71	2-7		60	53	64	61	50	44
		72	2-4		67	64	84	65	50	45
		73	5-3		68	57	68	70	49	45
		74	9-5		46	62	67	67	53	41
		75	10-2		44	54	57	56	41	33
		76	11-4		43	53	71	71	49	44
		77	4-1		48	—	76	62	56	51
		78	7-4		46	—	65	63	54	42
Avg					54	57.9	69.4	65+	50	44
Slag		79	1-11, 1-8		49	55	73	65	49	46
		80	1-18		45	62	68	61	46	43
		81	6-2		48	—	67	71	51	46
		82	9-8		48	—	66	69	50	41
		83	10-3		50	63	63	62	34	33
		84	11-3		46	60	63	70	49	44
		88	2-5		46	52	61	58	45	38
		89	3-4		56	69	82	57	46	38
		90	6-3		52	70	73	59	44	37
Avg					48.9	61.6	68.4	65-	47	42
Argillite		41	1-1		37	45	62	63	42	40
		42	1-17, 1-19		60	45	76	71	49	44
		63	3-3		60	—	81	61	33	27
		64	7-3		60	77	73	64	48	37
		65	6-5		56	67	67	42	44	35
		66	4-2		58	—	80	62	56	51
Avg					55.2	58.5	73.2	64	45	39
Diabase		67	6-2		44	—	58	46	37	31
		68	6-4		45	—	57	53	37	30
Avg					45		58	49	37	31
Gneiss		40	1-14		36	—	56	56	43	40
Sandstone		86	2-2		53	65	71	69	54	49
		87	5-2		53	67	77	73	51	48
Avg					53	66	74	71	53	49
Quartzite		85	1-23		46	—	69	54	46	42
Siltstone		45	2-9		41	51	71	58	51	45

Note: 1 in. = 25.4 mm.

[a]Were considered to be calcareous sandstone by Pennsylvania DOT petrographers.
[b]In Pennsylvania, consist of mostly (65 to 90 percent) sandstone or siltstone material (2).

Figure 5. Polishing results of various laboratory procedures on limestone aggregates.

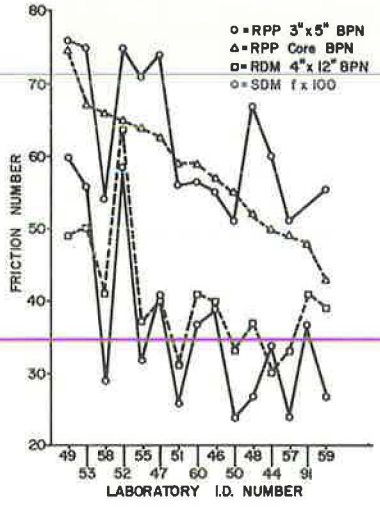

Table 3. Correlation coefficients for laboratory polishing results.

Sample	Method		Polished Core, RPP (BPN)	3 by 5-In. Panel, RPP (BPN)	4 by 12-In. Panel, RD (BPN)
	Polishing	Measurement			
3 by 5-in. panel	RPP	BPN	0.58	—	0.71
4 by 12-in. panel	RDM	BPN	0.64	0.71	—
4 by 12-in. panel	RDM	DTN	0.51	0.91	0.60
10 particles	SDM	f × 100	0.70	0.77	0.82

Note: 1 in. = 25.4 mm.

Figure 5. A polished-core BPN was plotted in descending order of magnitude against the aggregate laboratory identification number. Results obtained by using the other methods were plotted in the same order as the cores for easy comparison. The rank method (7) was used to correlate each two sets of results, and the correlation coefficients are given in Table 3.

Figure 4 shows that the various polishing methods and friction measurement procedures resulted in different frictional number levels and ordering of the aggregates tested. However, all methods seem to indicate similar trends in evaluating the polishing characteristics of the aggregates. The coefficients of correlation given in Table 3 varied from poor to fairly good, and this indicated the degree of similarity between results obtained by using one method or the other. Of particular interest are the fair correlations obtained between results of polishing individual aggregates by the exploratory SDM and the other methods. The encouraging results seem to imply that, with further possible improvements, particularly on sample preparation, the SDM may become an expedient method for determining aggregate frictional properties.

COMPARISON OF LABORATORY AND FIELD SKID TEST RESULTS

Data Used in Comparison

A few weeks after construction, field skid measurements were made periodically on the test sections by Pennsylvania DOT according to ASTM E 274. These data, covering from 1968 through 1973, were supplied together with aggregate petrographic classification, insoluble residue for the carbonates, average daily traffic (ADT) and average daily truck traffic (ADTT) obtained after construction, and pavement surface temperature at the time of testing. Skid numbers (SN) were also corrected for temperature to a base of 70 F (21.1 C) at the rate of ±3 SN/10 F (3 SN/5.6 C). These and other details of the test strip program are contained in department reports (1, 2). Reduction of the data to a form usable in this phase of the research was made and tabulated by type of aggregate, as is given for limestone in Table 4.

Since considerations of safe highway travel demand examination of the worst (most polished) surface condition, the annual minimum SN for each section was extracted from the data. Values obtained for replicate sections were generally close enough to justify averaging. Average values were calculated and tabulated, and, for each replicate pair (or more) or sections, the average was plotted in two curves, one for temperature-corrected and one for uncorrected values (8). Furthermore, because SNs have been found to vary with time (season and year), traffic, and other conditions of testing (1, 2, 9, 10), the average of the last 3-year minimum average SNs was calculated. We consider this average to represent a realistic, unbiased average minimum value of the steady-state frictional properties of surface aggregates after the pavement had relatively stabilized. The 3-year minimum average SN, the absolute minimum SN, core BPN, and percentage drop (from initial to polished) in SN and BPN are also given in Table 4.

Laboratory-Field Data Correlation

For all the aggregates and sections used in the test strips, BPNs on laboratory-polished pavement cores were correlated with SN_{40}. Previously (6), correlations between polished-core BPN and mean SN through 1971 resulted in poor coefficients ranging from 0.35 to 0.50. This time, correlations were attempted between polished-core BPN and minimum SN and between core BPN and the 3-year minimum average SN. Both correlations were only fair and resulted in coefficients of 0.67 and 0.69 respectively. The latter correlation, BPN versus 3-year minimum average SN, is shown in Figure 6. Correlations between field data and laboratory polishing tests on aggregate panels resulted in a similar trend but in fewer satisfactory correlations having coefficients rang-

Table 4. Skid test data for limestone test strip sections.

Test Section	Percentage of Insoluble Residue	ADT/ADTT	Annual Minimum SN_{40}								Percent Drop[a]	1973 Vehicle Passes	BPN on Cores		
			Initial	1969	1970	1971	1972	1973	Avg 1971-73	Absolute Minimum			Unpolished	Polished	Percent Drop[b]
2-1	6.3	1,130/102	58	46	49	35	52	39	42	35	39.6	2,160,000	70	51	27.1
2-3	6.3	1,130/102	48	48	53	35	48	35	39	35	27.1	2,160,000	66	48	27.3
2-8	6.3	1,130/102	50	52	58	39	51	40	43	39	22.0	2,160,000	71	51	29.2
3-1	10.1	15,700/804	35	28	34	27	31	32	30	27	26.7	24,580,000	61	47	23.0
3-2	1.5	15,700/804	30	21	31	22	28	30	27	21	30.0	24,730,000	63	48	23.8
4-4	2.1	1,900/374	63	65	53	39	50	38	42	38	39.7	3,120,000	74	66	10.8
5-1	2.8	5,000/377	51	45	50	41	44	41	42	41	19.6	9,530,000	66	57	13.6
5-4	24.1	5,000/377	51	47	52	45	50	44	46	44	13.7	9,490,000	74	63	14.9
6-1	0.8	5,500/568	42	28	43	36	37	25	33	25	40.5	8,810,000	58	43	25.9
7-5	7.1	4,500/252	58	68	37	50	46	34	44	34	41.4	6,920,000	68	58	14.7
8-1	37.4[c]	625/129	51	47	64	60	51	52	54	47	7.8	1,130,000	77	75	2.6
8-3	8.6	625/129	46	42	49	43	45	44	44	42	8.6	1,130,000	67	51	23.9
9-1	3.7	4,243/299	49	35	46	40	39	35	38	35	28.6	8,050,000	71	59	16.9
9-6	1.0	4,243/299	53	35	45	45	42	35	41	35	33.9	7,910,000	74	55	25.7
10-1	35.5[c]	4,676/168	49	47	43	38	38	38	38	38	22.4	8,850,000	75	65	13.3
10-4	38.4[c]	4,676/168	45	38	46	34	38	37	36	34	24.4	8,850,000	74	67	9.5
11-1	1.2[d]	3,813/288	64	48	57	49	49	41	46	41	35.9	7,060,000	77	64	16.9
Avg			49	44	48	40	43	38	40	35	28.6		70	57	18.6

[a]Initial to minimum. [b]Initial to polished. [c]Loyalhanna. [d]Ohio.

Figure 6. Polished-core BPN versus 3-year minimum average SN_{40} on all sections.

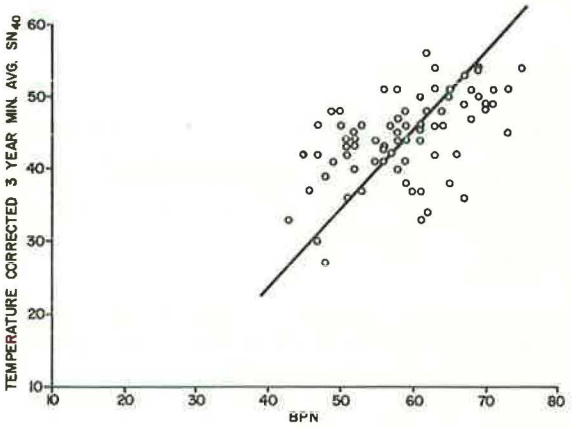

Figure 7. 3-year minimum average SN_{40} versus 5-year absolute minimum SN_{40} on all sections.

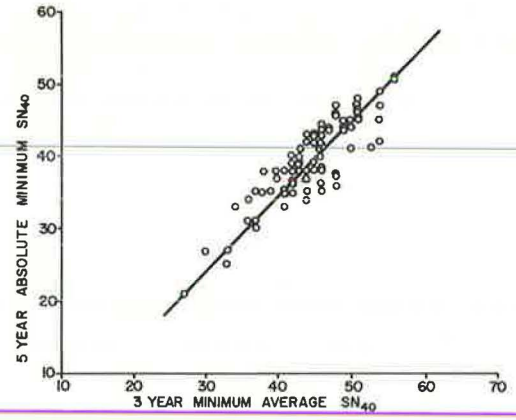

Figure 8. Temperature-corrected versus uncorrected 3-year minimum average SN_{40} on all sections.

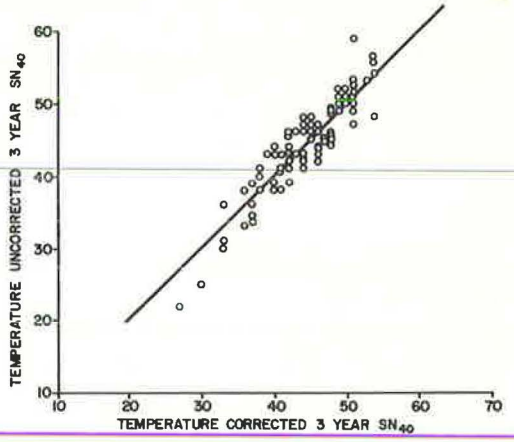

ing from 0.55 to 0.65.

Similar correlations obtained from using minimum SN and 3-year minimum average SN encouraged us to find whether correlations existed between these two parameters, when used in either the temperature-corrected or the uncorrected form. Figure 7 shows the correlation between the temperature-corrected 3-year average SN and the absolute minimum SN for all test sections, and Figure 8 shows corrected versus uncorrected 3-year minimum average SN for the same sections. It is apparent from the figures that, in both cases, good correlations ($r > 0.90$) and close relationships existed between the parameters. Generally, the 3-year minimum average SN is about five skid numbers higher than the absolute SN, but temperature-corrected and uncorrected SN have approximately a 1:1 relationship. Accordingly, only one set of data representing any of these parameters needs to be used in subsequent correlations.

Other attempts included a correlation between polished-core BPN and minimum SN for the carbonate sections only. The scatter of data points and the coefficient for this correlation were even worse than for the similar correlation of data for all sections; this probably indicated the large variability between aggregates within the carbonate group and pointed to the need for investigating individual carbonate aggregates on their individual merit, although as a group they seem to fall into the poor to marginal performance category.

Several factors could have contributed to the generally unsatisfactory correlation results obtained between laboratory and field frictional numbers. These factors include, but are not limited to, basic differences in measurement method and testing speed (10) and probable variations between core and field surface texture due to local variations and field surface changes caused by climatic changes and increased use of studded tires. Therefore, in the future, BPNs should also be measured in the field simultaneously with SN measurements, if some good correlations are to be achieved.

In the past decade or so, several attempts have been made to correlate portable testers and skid trailers (11, 12, 13). Correlation results have ranged from poor to fair or good, but there seems to be no general agreement among researchers on a resulting regression equation or set of equations that can be used with confidence.

Comparison and Ranking of Aggregates

All aggregates used in this research were grouped into 10 general types (Table 1). For a comparison of aggregates by type, the annual minimum SN for all sections in each group were averaged (Table 4). For each type, an average curve representing the group by type was plotted, as shown in Figure 9. These curves show the performance of each aggregate type. However, variations within each type due to the spread of data around the average ranged from fairly small (about ±3 SN) for dolomites, to very large (about ±12 SN) for limestones. Furthermore, the zigzag pattern of some curves makes definitive ranking of the aggregates by this procedure very difficult. Accordingly, another approach had to be followed.

For a ranking of the aggregates by each type, the 3-year minimum average SN, the absolute minimum SN, and the polished-core BPN values were pooled and averaged, and this resulted in one grand average of each friction number per aggregate type. These average values are given by aggregate type in Table 5. To indicate the extent of variation from the average value, the range around each average was also recorded in Table 5. One parameter had to be used as reference for the ranking. The 3-year average was chosen for reasons that have been discussed. Ranking of the aggregates was now attainable by the three parameters, and ranking results appear in both Table 5 and Figure 10. The obvious anomalies or suspicious deviations were given in the notes to Table 5.

Correlation of Ranking Data

From Figure 10 and Table 5, one can see that the 3-year minimum average and the

Figure 9. Average minimum SN for five aggregate types.

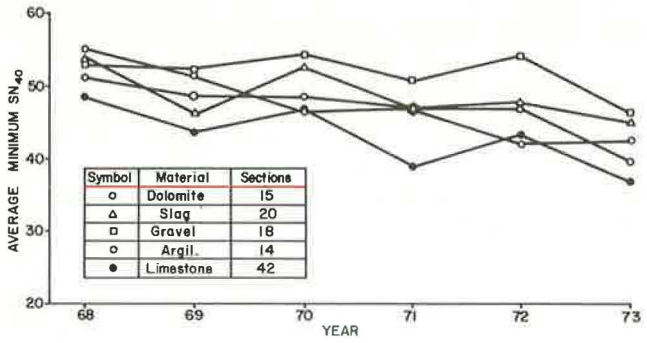

Table 5. Ranking of aggregates used in test strips.

Aggregate	Number of Test Sections	3-Year Minimum Average SN_{40} SN	Range	Rank	5-Year Minimum Average SN_{40} SN	Range	Rank	Polished Core BPN BPN	Range	Rank[a]	Rank[b]
Sandstone	4	52	51 to 54	1	48	48 to 49	1	71	69 to 73	1	1
Siltstone	2	51	48 to 54	2	45	42 to 48	2	58	54 to 62	5	5
Gravel	18	50	41 to 56	3	44	33 to 51	3	65+	56 to 71	2	2
Gravel[c]	16	51	49 to 56	3[d]	45	41 to 51	3[d]	66	61 to 71	2[d]	2[d]
Slag	20	47	34 to 51	4	42+	33 to 47	4	65-	57 to 71	3	3
Slag[e]	18	48	44 to 51	4[d]	43	38 to 47	4[d]	65	57 to 71	3[d]	3[d]
Quartzite	2	46+	43 to 49	5	42-	39 to 45	5	54	52 to 56	8	7
Argillite	14	45	33 to 54	6	39+	27 to 51	7	64	52 to 73	4	4
Argillite[f]	12	46	42 to 54	6[d]	41	35 to 51	6[d]		52 to 73	4[d]	4[d]
Dolomite	17	44	40 to 48	7	39-	36 to 43	8	52	45 to 64	9	9
Gneiss	2	43	41 to 45	8	40	39 to 42	6, 7[d]	56	54 to 58	7	6
Diabase	6	41	37 to 48	9	36	30 to 47	9	50	46 to 53	10	10
Diabase[g]		48		4[d]	47		4[d]		—		
Limestone[a]	42	40	27 to 54	10	35	21 to 47	10	57	43 to 75	6	
Limestone[b]	39	39	27 to 46	10	34	21 to 44	10	54	43 to 64	—	8

[a]Including six sections of Loyalhanna formation, considered calcareous sandstone by Pennsylvania DOT petrographers.
[b]Excluding six sections of Loyalhanna formation, considered calcareous sandstone by Pennsylvania DOT petrographers.
[c]Excluding section 10-2, which had fine grained material and very dense mix that tends to decrease skid resistance (2).
[d]Alternate rank.
[e]Excluding section 10-3, which consistently had an anomalously low SN attributed, at least in part, to excess asphalt content (2).
[f]Excluding section 3-3 in which the coarse aggregate contained 60 percent sericite (very fine-grained mica—Moh's number, H=2) that is suspected of contributing to the low SN for this section.
[g]Two sections (1-21 N and S), where the fine aggregate was also diabase; other sections (6-2 and 6-4) had limestone as the fine aggregate.

Figure 10. Ranking of aggregates based on field and laboratory data.

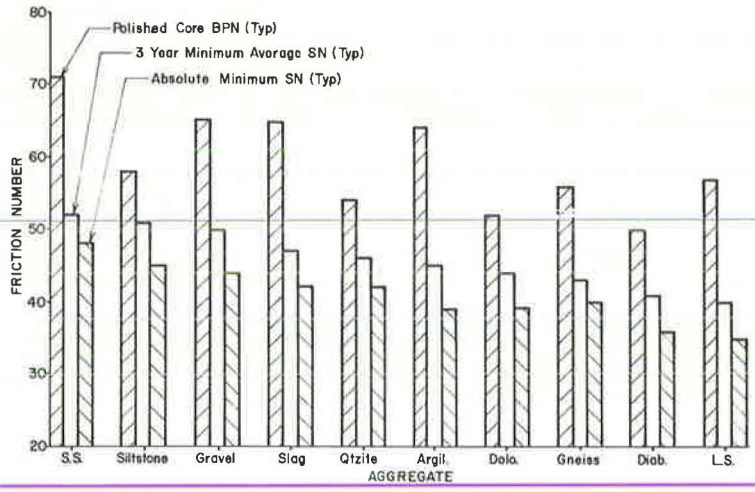

absolute minimum SNs ranked the aggregates in approximately the same order, but a different ranking resulted when core BPN values were used. This follows the lack of good correlations between BPN and SN, as has been discussed. However, correlations between core BPN and SN by aggregate type, as shown in Figure 11, resulted in relatively high coefficients (r = 0.85 by the rank method for Figure 11), and this indicated that at least a general trend exists in ranking aggregate types by both laboratory and field methods. Similar correlations using other laboratory-polished samples and SNs followed a similar pattern with coefficients ranging from 0.75 to 0.85.

Another approach was to correlate the percentage drop in the core BPN with the percentage drop in SN, as shown in Figure 12. The resulting coefficient of correlation was slightly less than 0.50; this indicated that the approach was unsatisfactory.

OTHER OBSERVATIONS ON BITUMINOUS PAVEMENT SKID RESISTANCE

Periodic Variations in Skid Resistance

Skid resistance was measured periodically on all test strip sections. SNs varied from period to period, probably because of changes in season and in environmental conditions of testing such as temperature, rainfall, and other weather-related factors, but SNs seemed to follow some cyclical annual pattern resembling a sine wave, as was observed by Gramling and Hopkins (1). However, in most cases, SN-time wear curves had a downward negatively sloping trend similar to laboratory polishing curves; this indicated a general decrease in the level of SN with passage of time and traffic until a leveling-off occurred. Minimum SNs generally occurred in the summer and fall, and the larger portion occurred from August through October, as may be seen in Figure 13. SN annual variation between minimum and maximum had a wide range for some aggregates like the limestone and a narrow range for other aggregates like the gravel and quartzite (2). In addition, high ADT caused more seasonal variation in SN than low ADT (1).

Previous research has reported that temperature does affect SN. Rates of change ranging from $<\frac{1}{2}$ to >3 SN/10 F ($<\frac{1}{2}$ to >3 SN/5.6 C) have been reported (10). However, there seems to be no general agreement among researchers on a correction factor. It may be that correction for temperature is not necessary in the ranking of aggregate performance, as was implied by Figure 8. However, it seems that more thorough research in this area is still needed, especially if corrective measures are to be taken when SN_{40} falls below an adopted arbitrary level.

Effect of Traffic on Skid Resistance

Traffic and aggregate characteristics have generally been recognized as the most important factors that influence pavement surface polishing (1, 10, 14). Some aggregate factors have already been discussed in this paper and elsewhere (15). As for traffic on any given surface, the higher the traffic is, the lower the skid number will be, as shown in Figure 14. The curves in Figure 14 represent actual test data on limestone test sections carrying different ADT.

In the laboratory, traffic is simulated by polishing equipment such as circular tracks, stationary rotating wheels, or reciprocating equipment (9, 11, 16). On laboratory-polished samples, frictional numbers generally deteriorate as cumulative polishing passes increase until a practically stable state is reached. In the field, pavement surfaces have been found to regain in SN level after some initial loss due to the polishing effect of traffic. Therefore, the question has been raised about whether ADT or accumulated vehicle passes should be considered in investigating SN deterioration. Both concepts have been used in skid-resistance investigations (1, 9, 12, 14), and claims have been made that one parameter or the other is the more dependable to use. In this research, it was found that both parameters, ADT and accumulated traffic, should be considered because both parameters appear to influence the level of skid resistance reached,

Figure 11. Polished-core BPN versus minimum SN_{40}.

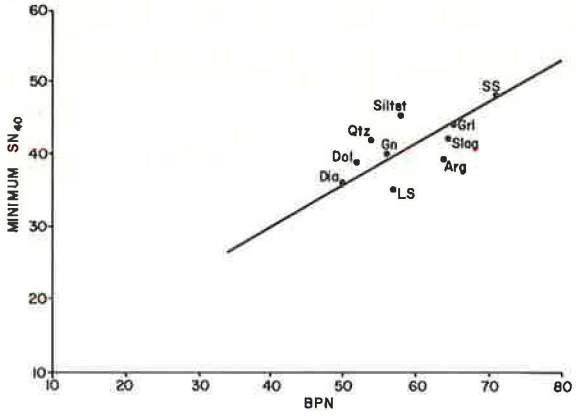

Figure 12. Percentage drop in core BPN versus percentage drop in SN_{40}.

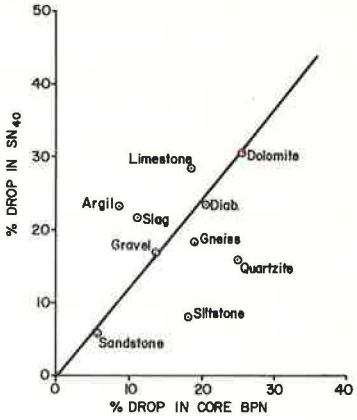

Figure 13. Frequency of occurrence of minimum SN_{40} versus time of year for 1969-73.

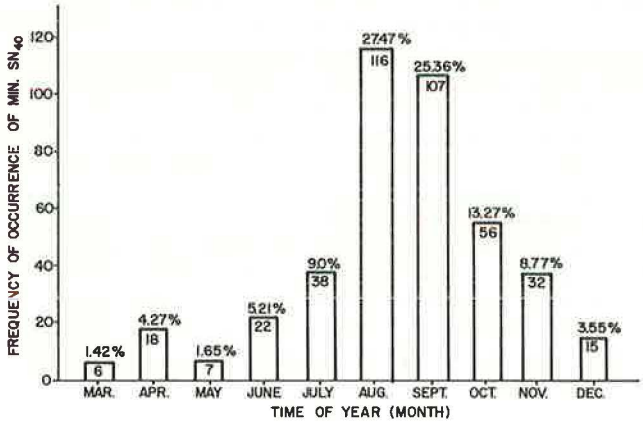

Figure 14. Effect of ADT on minimum SN over limestone surfaces.

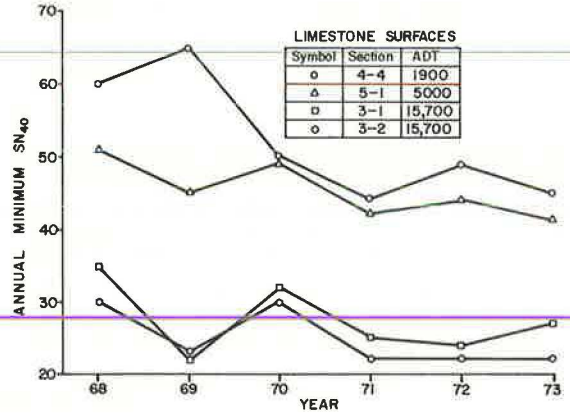

as may be seen from Figures 15 and 16 for ADT and cumulative traffic respectively.

Figure 15 shows that similar correlations are obtained between 3-year SN and ADT, and between 3-year SN and ADT (truck). Furthermore, at 3-year SN = 40, the effect of an average truck on pavement polishing is equivalent to about 18 passenger cars. This equivalency varies depending on at what SN level it is estimated, but the ratio of 1:18 taken at SN = 40 represents an average value. Similar correlations using all the test sections resulted in similar equivalencies. Furthermore, slopes of curves using data from all sections resulted in about a 1:20 ratio.

From Figure 16, one can see that the 3-year average SN generally deteriorates as the number of vehicle passes increases, despite intermediate recoveries due to surface rejuvination. From charts like Figure 16, drawn for a particular type of surface and aggregate, one can estimate the number of vehicle passes that a pavement will be expected to endure before a predetermined minimum SN is reached. The rate of SN deterioration with accumulated traffic can also be estimated for a given surface and aggregate.

Insoluble Residue and Skid Resistance

Earlier research has indicated that skid resistance of the carbonate aggregates increases as the portion of insoluble residue in the aggregate increases. Quantitative relationships have been sought between the two parameters, and several have been reported (2, 17, 18). But there seems to be neither general agreement on the percentage of residue that will produce a predetermined minimum SN nor on the rate of increase of SN as the percentage of residue increases.

In this research, an attempt was made to correlate both laboratory BPN on cores and field 3-year minimum average SN with the percentage of insoluble residue. The correlations are shown in Figure 17. The wide scatter of data in the figure indicates unsatisfactory quantitative relationships between the residue and the frictional number. However, there appears to be a trend of increase in both the laboratory and the field frictional numbers as the percentage of residue is increased. It appears that the influence of residue may be more pronounced in laboratory polishing than it is in the field. Figure 17 shows that carbonate samples having residue distributed at 2 to 5 percent intervals in the range of 10 to 35 percent are needed to produce sufficient data points. The implication is that a more thorough investigation covering these intermediate levels of insoluble residue will be needed before definitive quantitative relationships between insoluble residue and SN can be established. If carbonates having residues in the 20 to 35 percent range can be shown to provide a significantly higher level of skid resistance than those with less residue, selective quarrying may enable some producers to meet higher levels of skid-resistance requirements.

SUMMARY AND CONCLUSIONS

The research discussed was part of a cooperative effort to evaluate bituminous pavement and aggregate polishing, both in the laboratory and in the field, and to investigate whether correlations of practical application existed between the two approaches. Influences of other factors encountered in the research process, such as environmental, traffic, and petrographic characteristics of surface aggregates, were also observed and reported on.

A test strip program containing 156 pavement sections in 11 different locations in Pennsylvania and incorporating various aggregates was initiated and monitored periodically for field skid resistance. Fifty-two aggregate samples and 223 pavement cores representative of the test sections were polished and tested for friction in the laboratory. Correlations were made between laboratory and field results. The following conclusions are supported by the findings from this research:

1. Different methods of laboratory polishing and friction measurement produce

Figure 15. ADT and ADTT versus 3-year minimum average SN_{40} grouped by ADT.

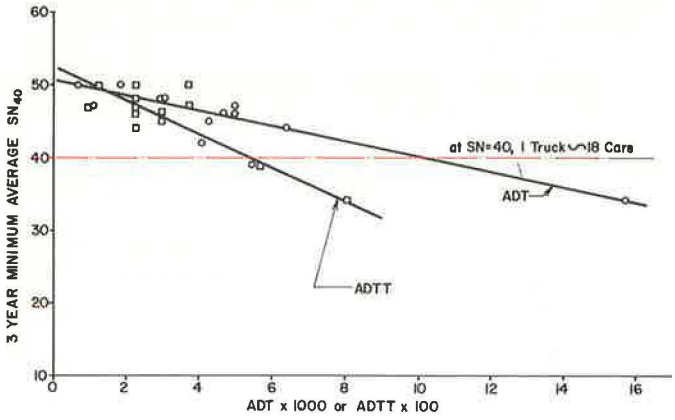

Figure 16. 3-year minimum average SN_{40} versus cumulative traffic on carbonate sections.

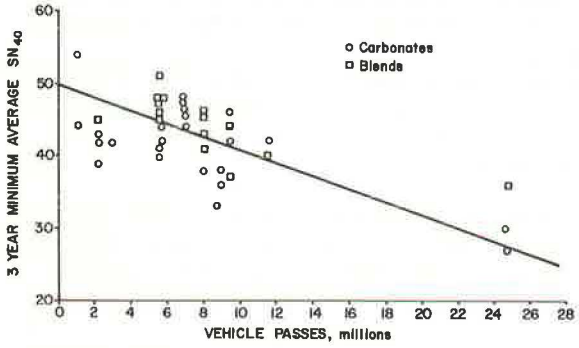

Figure 17. Percentage of sand-size insoluble residue versus friction number.

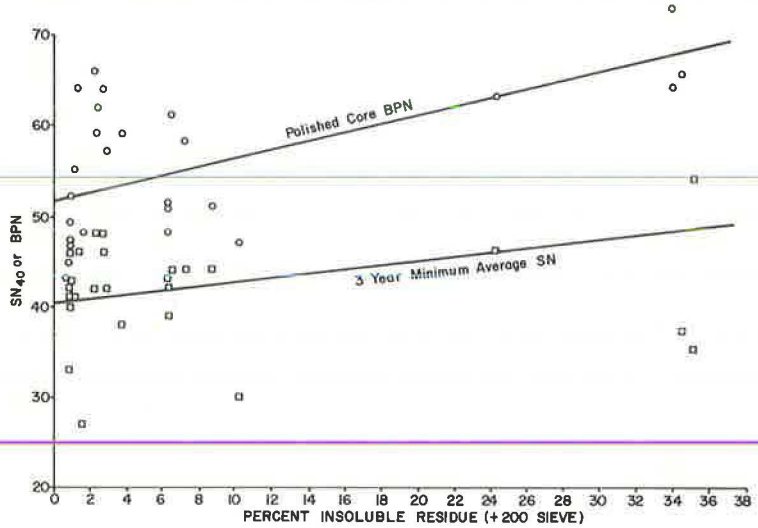

different friction number levels and do not always rank the tested aggregates in the same order; however, they do indicate similar general trends and predict similar general levels of aggregate resistance to polishing.

2. The exploratory SDM seems to be useful for expedient laboratory evaluation of aggregate polishing characteristics.

3. Correlations between laboratory and field data indicate similar trends in polishing characteristics, but they do not produce, through regression equations, satisfactory mathematical relationships that can be applied with confidence for the prediction of specific numerical values of field SN based on laboratory-measured SN.

4. Field and laboratory methods rank aggregates in a closely similar order, but not always in the same order; therefore, a specific correlation should always be established between the particular method to be used for laboratory and field SNs.

5. Minimum SNs correlate significantly better than mean SNs with laboratory-polishing results. No significant difference in analysis seems to result whether an absolute minimum or 3-year minimum average SN is used. Both rank aggregates in practically the same order.

6. Temperature-corrected and uncorrected minimum SNs rank aggregate performance similarly, when used in skid-resistance analysis.

7. Minimum SNs generally occur in the late summer and fall of the year and predominate in August through October.

8. Percentage drop in frictional number between the initial and the polished condition is not a good indicator of pavement or aggregate skid-resistance performance.

9. On any given surface, the higher the ADT is, the lower the skid-resistance levels will be. For any ADT and surface, the skid-resistance level fluctuates widely at first but stabilizes and levels off after about 2 years of service; and for a given ADT, the skid-resistance level is lower on some aggregates like limestones than on others like gravels.

10. There seems to be an equivalency in polishing effects between trucks and passenger cars. One truck appears to be equivalent to about 18 cars.

11. Until a pavement surface stabilizes, skid-resistance level decreases with passage of time and traffic, mainly because of accumulated traffic action.

12. In this research, increase in portions of insoluble residue gave only general trends of increase in skid resistance. Further tests are needed on samples that will cover narrow intervals in the range of 10 to 35 percent insoluble residue content.

13. Where the more polish-susceptible aggregates interact with high traffic volumes to produce a pronounced seasonal cyclic pattern of skid resistance, a procedure should be developed for predicting minimum SN from field tests taken at any time during the cycle.

ACKNOWLEDGMENTS

This research was sponsored by the Pennsylvania Department of Transportation in cooperation with the Federal Highway Administration. The work was performed at the Pennsylvania Transportation Institute, Pennsylvania State University. Progress of the research was aided by many of the personnel of Pennsylvania DOT and FHWA, as well as by several Pennsylvania State University faculty, staff, and students.

The contents of this paper reflect the views of the authors, who are responsible for the facts and the accuracy of the data presented. The contents do not necessarily reflect the official views or policies of the Pennsylvania DOT or FHWA. This paper does not constitute a standard, specification, or regulation.

REFERENCES

1. W. L. Gramling and J. G. Hopkins. Skid Resistance Studies—Aggregate-Skid Resistance Relationship as Applied to Pennsylvania Aggregates. Pennsylvania Department of Transportation, final rept., May 1974.

2. M. A. Furbush and K. E. Styers. The Relationship of Skid Resistance to Petrography of Aggregates. Pennsylvania Department of Transportation, final rept., July 1972.
3. H. W. Kummer. Research Equipment for the Study of Rubber Friction and Skid Resistance. Pennsylvania State Univ., Rept. J11, 1966.
4. W. G. Mullen, S. H. Dahir, and B. D. Barnes. Two Laboratory Methods for Evaluating Skid Resistance Properties of Aggregates. Highway Research Record 376, 1971, pp. 123-135.
5. A. K. Stiffler. Relationship Between Wear and Physical Properties of Roadstones. HRB Special Rept. 101, 1969, pp. 56-69.
6. R. R. Hegmon and W. E. Meyer. Laboratory Polishing of Pavement Cores and Comparison With Field Performance. Automotive Research Program, Pennsylvania State Univ., Rept. S52, 1972.
7. Chemical Rubber Company. Standard Mathematical Tables, 1965.
8. S. H. Dahir and W. E. Meyer. Bituminous Pavement Polishing. Pennsylvania State Univ., final rept.
9. Automotive Research Program Publications. Pennsylvania State Univ., Rept. S25, 1974.
10. H. W. Kummer and W. E. Meyer. Tentative Skid Resistance Requirements for Main Rural Highways. NCHRP Rept. 37, 1967.
11. Proc., 1st International Skid Prevention Conference, Charlottesville, Va., 1969.
12. Synthesis of Highway Practice—Skid Resistance. NCHRP Rept. 14, 1972.
13. W. G. Mullen. Prediction of Pavement Skid Resistance From Laboratory Tests. Transportation Research Record 523, 1974, pp. 40-55.
14. W. S. Szatkowski and J. R. Hosking. The Effect of Traffic and Aggregate on the Skidding Resistance of Bituminous Surfacings. U.K. Transport and Road Research Laboratory, TRRL Rept. LR 504, 1972.
15. S. H. Dahir and W. G. Mullen. Factors Influencing Aggregate Skid-Resistance Properties. Highway Research Record 376, 1971, pp. 136-148.
16. W. A. Goodwin. Pre-Evaluation of Pavement Materials for Skid Resistance—A Review of U.S. Techniques. HRB Special Rept. 101, 1969, pp. 69-80.
17. J. E. Gray and F. A. Renninger. Limestones With Excellent Non-Skid Properties. Crushed Stone Journal, Vol. 35, No. 4, 1960, pp. 6-11.
18. W. C. Sherwood and D. C. Mahone. Predetermining the Polish Resistance of Limestone Aggregates. Highway Research Record 341, 1970, pp. 1-10.

PAVEMENT SKID-RESISTANCE REQUIREMENTS

Duane F. Dunlap, Paul S. Fancher, Jr., Robert E. Scott, Charles C. MacAdam, and Leonard Segel, Highway Safety Research Institute, University of Michigan, Ann Arbor

Requirements for pavement skid resistance are determined in relation to roadway design elements, tire-tread depth, and rainfall experience. Turnpike accident data are analyzed to show that certain low-curvature curves have higher than average accident involvement histories, and excessive water build-up and, hence, poor pavement drainage is determined to be a responsible factor. Tire traction is shown to be substantially degraded at water depths well below those needed for hydroplaning, and water depth on the road surface is shown to be primarily influenced by road width, superelevation, and rainfall rate and to be essentially independent of grade. We used computer simulation analyses involving parametric variations of vehicles, tires, road surfaces, curvature, superelevation, grade, and maneuvers to define specific limiting velocity boundaries for vehicle-handling performance and then used the accident, traction, drainage, and vehicle performance analyses to develop an equation for required pavement skid number. An example is used to illustrate applications of the equation.

•A SKID number of 37 was recommended by Kummer and Meyer (1) as the minimum requirement for main rural highways in 1967. This recommendation was based on the normal skid-resistance needs of traffic as derived from driver behavior studies. In this paper, the development of skid-resistance requirements is taken a step further, and such requirements are related directly to roadway design elements, tire characteristics, and precipitation experience. The work reported on is an outgrowth of studies conducted for the National Cooperative Highway Research Program concerning the influence of combined highway grade and horizontal curvature on skidding accidents (2). The studies involved the analysis of accident data, vehicle loss-of-control mechanisms, pavement drainage, and tire-pavement friction.

ACCIDENT DATA ANALYSIS

Accident data for the Ohio and Pennsylvania Turnpikes were analyzed to determine the relationship between roadway design elements and accident rates. Neither set of data was found to markedly depend on grade, although the accident rates for downgrades were higher than for upgrades. Accident rates did increase as curvature increased. Figure 1 shows that 1-deg curves on the Ohio Turnpike were found to have a high accident rate; this was particularly true during wet weather. On one specific 1-deg curve on a 3-deg downgrade, almost 70 percent of the accidents occurred during wet weather. Heavily worn tires were associated with many of these accidents; however, no evidence of effects that could be attributed to combinations of curvature and grade was found.

TIRE-PAVEMENT TRACTION AND WATER DEPTH

Water depth has a critical influence on the friction available at the tire-pavement interface. Tire hydroplaning is commonly considered to be the primary adverse effect resulting from excess water on the pavement. Actually, however, most wet-weather skidding accidents undoubtedly occur as a result of water depths well below those

needed for hydroplaning (3).

Equations for predicting pavement water depth as a function of rainfall rate and pavement surface geometry have been independently developed through research at the Texas Transportation Institute, the U.K. Transport and Road Research Laboratory, and the Goodyear Tire and Rubber Company. These equations show that rainfall rate, pavement width, and superelevation are the primary factors influencing water depth. Roadway grade and pavement texture are secondary factors. [A physical explanation of why superelevation is an important factor and grade is not can be found elsewhere (2).] The most conservative of these equations (4) (i.e., for predicting the greatest depths of water) can be written as follows:

$$d = (5.9 \times 10^{-3}) \left(\frac{LI}{e}\right)^{0.47} (e^2 + G^2)^{0.135} \quad (1)$$

where

d = water depth above the pavement texture in inches (millimeters),
L = pavement width in feet (meters),
e = pavement superelevation in feet/foot (meters/meter),
G = percentage of pavement grade, and
I = rainfall intensity in inches/hour (millimeters/hour).

SKID-RESISTANCE REQUIREMENTS

Computer simulation was used to examine parametric variations of road (surface, curvature, grade, and superelevation) and tire factors in three types of vehicle maneuvers. These results were then generalized to yield pavement skid-resistance requirements.

The maximum velocities at which these maneuvers could be performed without loss of control were used as measures to quantify the results. These velocities and maneuvers are defined as follows:

V_{CR} = limiting velocity (i.e., without loss of control) for traversing a curve; drive thrust is applied to maintain constant velocity.
V_{LC} = limiting velocity for traversing a curve while, at the same time, a 9 to 12-ft (2.7 to 3.7-m) lane-change (obstacle-avoidance) maneuver is performed; drive thrust is applied to maintain constant velocity.
V_{LOC} = maximum initial velocity from which a combined lane-change and abrupt-stop maneuver can be performed while a curve is traversed.

The simulation results showed that executing a lane change on a curve (i.e., toward the inside of the curve) generally requires that more lateral force be generated in the tire-road friction couple than a similar maneuver on a tangent section requires. In normalized units, the additional force margin can be denoted as follows:

$$\bar{f} = \frac{V^2 D}{85{,}944} - e \quad (2)$$

where

V = maximum velocity at which the lane change can be executed in miles (kilometers) per hour, and
D = curvature of the curve in degrees.

It is evident, then, that an extra margin of maneuvering safety should be built into curved sections of the roadway. It is reasonable to provide this margin by increasing the skid number (SN) on a curve over that needed on a tangent section by an amount proportional to $\bar{f}$.

Similarly, considering that downgrades tend to correlate with an increase in the accident rate (physically a vehicle's weight shifts forward on a downgrade; this results in an increased potential for rear-wheel lockup during braking and, hence, in a tendency for directional instability or spinout), it seems reasonable to allow an independent SN margin for downgrade sites proportional to the magnitude of the downgrade. At curve-grade sites, then, the requirements for skid resistance can be combined additively to obtain the following expression for required SN:

$$SN_{CG} = SN_T + 100(\bar{f} + G') \tag{3}$$

where

SN_T = required SN for safe travel on a tangent section,
G' = magnitude of the grade for downgrades, and
G' = 0 for upgrades.

Equation 3 can be modified to account for deficiencies in pavement drainage and for the influence of tire characteristics different from that of the ASTM standard tire. (The ASTM standard tire is used as a reference because it is the standard tire used in pavement skid-resistance measurements.) This modification is as follows:

$$SN_{CG} = \frac{SN_T + 100(\bar{f} + G')}{T_F} + SN_D \tag{4}$$

where

SN_D = SN increment needed to overcome drainage deficiencies, and
T_F = factor to relate operational tire characteristics to the ASTM standard tire.

Equation 4 can be further modified to yield an expression for the required SN, measured at 40 mph (64 km/h), for safe travel at velocity V. The result is as follows:

$$SN_{(40/V)CG} = \frac{SN_{(40/V)T} + 100(\bar{f} + G')}{T_F} + SN_D \tag{5}$$

where V is a characteristic velocity that is near the maximum velocity that vehicles travel on the given highway section. Examples of this velocity are the speed limit, the highway design speed, or the 90th percentile of the speed distribution.

Values of $SN_{(40/V)T}$ can be determined from the V_{LOC} curves in Figure 2. Through a process of normalizing the data on Figure 2 for curvature, grade, tire-tread depth, and SN gradient, it can be shown that

$$SN_{(40/V)CG} = \frac{SN_{(40/40)T} + 100(\bar{f} + G') + (0.2 - SN_{grad})(V - 40)}{T_F} + SN_D \tag{6}$$

where

$SN_{(40/40)T}$ = SN_{40} value needed on a tangent section for safe travel on ASTM equivalent tires at 40 mph (64 km/h) (this value is about 4 in equation 6), and
SN_{grad} = SN gradient, SN/mph (SN/km/h) (SN_{grad} is almost always negative).

Equation 6 is the desired relationship for SN requirements and is applicable only to main rural highways where the selected characteristic velocity is at least 50 mph (80 km/h).

APPLICATION

A careful examination of equation 1 shows that pavement water depth can be essentially expressed in terms of the rainfall rate I and the single drainage design parameter K(L/e), where K is a correction factor for overall slope. This parameter is plotted versus rainfall rate as shown in Figure 3. Figure 3 is divided into four parts by curves for design water depths of 0.02, 0.04, and 0.06 in. (0.51, 1.02, and 1.52 mm). A maximum design water depth of 0.02 in. (0.51 mm) is desirable because this is the standard depth used in pavement skid testing. In the acceptable region (Figure 3), where the design water depth is 0.02 in. (0.51 mm) or less, an increase in SN is not needed [0.02 in. (0.51 mm) is the standard water depth used in pavement skid testing]. Compensating increases recommended for other parts of Figure 3 are given below (1 in. = 25.4 mm):

Region in Figure 3	Design Water Depth (in.)	Skid Resistance Increment (SN)
Acceptable	0 to 0.2	0
Region I	0.02 to 0.04	7
Region II	0.02 to 0.06	13
Unacceptable	>0.06	Not recommended

Note that design water depths greater than 0.06 in. (1.52 mm) are not recommended since hydroplaning may occur at these depths.

When Figure 3 is used, rainfall rates between 0.25 and 0.50 in./hour (6.4 and 12.7 mm/hour) should be used for design purposes, depending on local precipitation experience. Rainfall rates greater than these values are relatively uncommon; they cause reduced visibility and, hence, a reduction in traffic speed. The slope factor K can be determined from Figure 4. T_F values (5) for use with Equation 6 are given below (1 in. = 25.4 mm):

Tread Depth (in.)	T_F
$^0/_{32}$, worn smooth	0.29
$^1/_{32}$	0.40
$^2/_{32}$	0.50
$^3/_{32}$	0.60
$^4/_{32}$	0.69
$^6/_{32}$, half worn	0.85
ASTM tire	1.00
$^{10}/_{32}$, new tire	1.20

Figure 1. Accident rate versus curvature for Ohio Turnpike, 1966 to 1970.

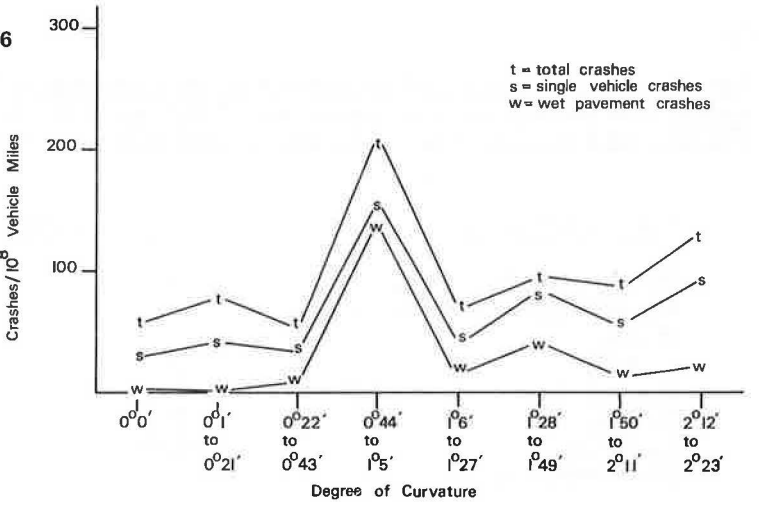

Figure 2. Effects of curvature and SN on V_{CR} and V_{LOC}.

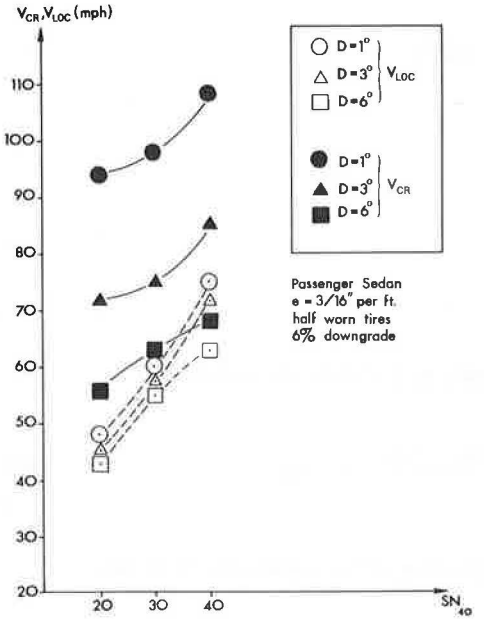

Figure 3. Drainage design parameter versus rainfall rate.

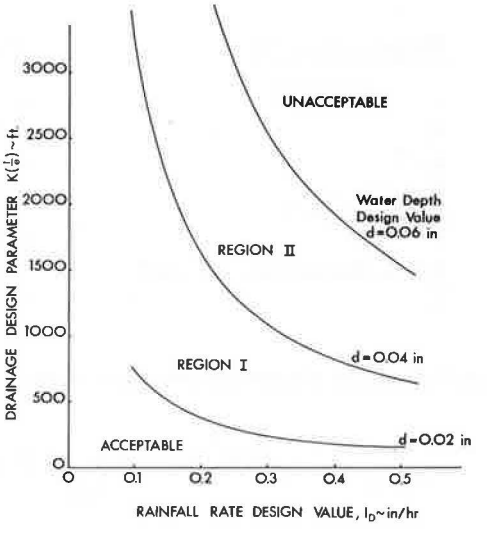

Figure 4. Slope factor versus pavement slope.

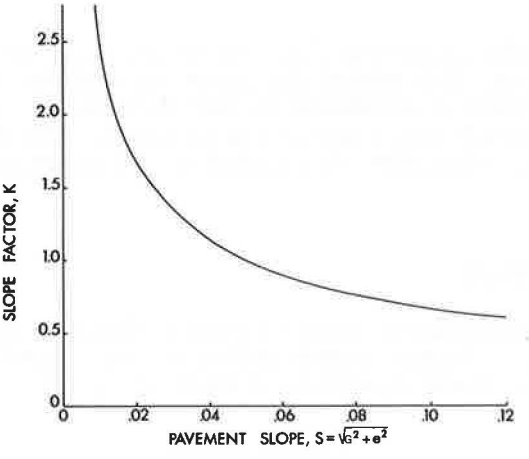

The site characteristics and measurements for an example of the use of equation 6 to specify skid resistance requirements are as follows (1 ft = 0.3 m, 1 in. = 25.4 mm, 1 in./ft = 83.3 mm/m, 1 mph = 1.6 km/h, 1 SN/mph = 0.6 SN/km/h):

Site Characteristic	Measurement
Roadway width, ft	24
Superelevated shoulder width, ft	10
D, deg	1
e, in./ft	3/8
G, percentage of downgrade	3
V, mph	80
I_D, in./hour	0.25
Tire-tread depth, in.	2/32

The derived quantities for an example of how equation 6 can be used are given below (1 ft = 0.3 m, 1 SN/mph = 0.6 SN/km/h):

Derived Quantity	Measurement
$S = \sqrt{e^2 + G'^2}$	0.0434
K	1.07
L, ft	30.5
K(L/e), ft	1,042
SN_D (region I)	7
$\bar{f}$	0.04
SN_{grad} (assumed), SN/mph	-0.5
T_F	0.50

Substituting the above derived quantities into equation 6 yields the following:

$$SN_{40/80} = \frac{4 + 100(0.04 + 0.03) + (0.2 + 0.5)(80 - 40)}{0.50} + 7 = 85 \quad (7)$$

If the tires were new (T_F = 1.2), then the corresponding SN_{40} value would be 40.

CONCLUSION

Equation 6 provides a practical means for determining the SN requirements for a given section of roadway. It is evident that geometry, drainage, and tire use enter into pavement skid-resistance requirements and that these factors lead to different skid-resistance needs on different sections of pavement. Although the data supporting equation 6 are not exhaustive, the equation is fully representative of the best available information.

ACKNOWLEDGMENT

This paper was developed as part of a National Cooperative Highway Research Program project (2) on the influence of combined highway grade and horizontal alignment on skidding. The work was carried out at the Highway Safety Research Institute, University

of Michigan. Harry A. Smith served as project engineer. The opinions, findings, and conclusions expressed in this paper are those of the authors and not necessarily those of the sponsoring agency.

REFERENCES

1. H. W. Kummer and W. E. Meyer. Tentative Skid Resistance Requirements for Main Rural Highways. NCHRP Rept. 37, 1967.
2. D. F. Dunlap, P. S. Fancher, R. F. Scott, C. C. MacAdam, and L. Segel. Influence of Combined Highway Grade and Horizontal Alignment on Skidding. Final Rept., NCHRP Project 1-14, Dec. 1973.
3. G. C. Staughton and T. Williams. Tyre Performance in Wet Surface Conditions. U.K. Transport and Road Research Laboratory, TRRL Rept. LR 355, 1970.
4. N. F. Ross and K. Russam. The Depth of Rain Water on Road Surfaces. U.K. Transport and Road Research Laboratory, TRRL Rept. LR 236, 1968.
5. P. S. Fancher, Jr., and L. Segel. Tire Traction Assessed by Shear Force and Vehicle Performance. Tire Science and Technology, Vol. 1, No. 4, Nov. 1973, pp. 363-381.

ACCIDENTS ON RURAL INTERSTATE AND PARKWAY ROADS AND THEIR RELATION TO PAVEMENT FRICTION

Rolands L. Rizenbergs, James L. Burchett, and Cass T. Napier,
Bureau of Highways, Kentucky Department of Transportation, Lexington; and
John A. Deacon, Department of Civil Engineering, University of Kentucky, Lexington

Friction measurements were made with a skid trailer at 70 mph (31 m/s) on 770 miles (1240 km) of rural, four-lane, controlled-access routes on Interstate and parkway systems in Kentucky. Each construction project was treated as a test section. Accident experience, friction measurements, and traffic volumes were obtained for each. Various relationships between wet-weather accidents and skid resistance were analyzed. Averaging methods were used to develop trends and minimize scatter. A moving average for progressively ordered sets of five test sections yielded more definite results. The expression of accident occurrence that correlated best with skid and slip resistance was wet-weather accidents per 100 million vehicle miles (161 million vehicle km). Accidents [at 70 mph (31 m/s)] increased greatly as skid numbers decreased from 27. Analysis of peak slip numbers and accident occurrences indicated similar trends.

•PAVEMENTS must be designed to have sufficient and enduring skid resistance to ensure safe highway travel in wet weather and to enable drivers to perform normal driving tasks without the risk of skidding or loss of vehicle control. In emergencies, a driver may be compelled to brake hard and, with conventional braking systems, may experience skidding regardless of how skid resistant the pavement may be. Antilocking brake systems minimize the risks of skidding and permit the driver to retain directional control of the vehicle. Without such a system, a vehicle will skid, and the driver potentially could loose control of the vehicle when the demand for braking force exceeds the tractive force. As friction (traction) increases, greater deceleration is available and a driver's chances of avoiding collision and remaining on the road are increased. Ideally, wet pavements should provide as much traction as dry pavements. In a practical and realistic sense, however, the question remains: What minimum level of friction should a pavement provide to safeguard the public from undue hazards associated with wet-weather driving? Little satisfaction is derived from merely maintaining a friction level at or near a critical value. The critical value, however, may serve as a criterion for posting wet-weather speed restrictions and for design of surface courses providing a due margin of safety.

Investigations elsewhere (1, 2, 3, 4, 5, 6) to establish minimum friction requirements fall into two categories: (a) studies of driver behavior and, therefore, frictional demands attending driving tasks and (b) analysis of accident data and accident experience as related to pavement friction. Studies in the first category represent a logical approach but involve extensive monitoring of representative driver populations under realistic roadway conditions and situations. Interpretations of what constitutes normal as opposed to emergency reactions or situations present a problem. Friction factors thus derived cannot easily be related to skid resistance measured with conventional testers (such as trailers) operated under prescribed procedures and test conditions.

Accident rates are higher on wet than on dry surfaces; many statistics are available to support this intuitive conclusion. Furthermore, research has shown that accident rates tend to increase as wet skid resistance diminishes. This relationship is now considered to be intuitive and a priori. However, the interaction of many contributing factors such as roadway geometrics, traffic characteristics, and driver behavior to-

gether with uncertainties about reliability and availability of accident data, type of friction measurements, and type of analysis has heretofore obscured relationships between accidents and pavement friction.

The primary objective of this study was to discern a relationship between accident experience and pavement friction for rural, four-lane, controlled-access roads on Interstate and parkway (expressway) systems in Kentucky. These highways were purposely chosen for this initial analysis because many of the usually confounding variables could be assumed to have minimal influence. Subsequent evaluations of such a relationship in conjunction with economical and technical considerations will surely guide the establishment of minimum levels of friction.

When a relationship between accidents and skid resistance is to be defined, the effect of all other parameters must be known or held constant insofar as possible. If the study is limited to rural, four-lane, Interstate and parkway facilities, some of the parameters, such as road geometrics, access control, and speed, may be assumed to remain reasonably constant. Traffic characteristics (volume and density) and pavement surface conditions (wet or dry and skid resistance when wet) are the regenerative and causative factors, respectively.

Annual average daily traffic (AADT) volumes were obtained for 1971. Accident data were those reported during 1970, 1971, and 1972. Pavement friction measurements were made between June and October 1971 on 770 miles (1240 km) of the Interstate and parkway systems. Both locked-wheel and peak slip resistances were measured. This peak resistance is often referred to as incipient friction and exceeds the resistance measured by the locked-wheel method. In normal driving, the vehicle operates in a preslip and cornering mode. Therefore, both locked-wheel skid resistance and peak slip resistance at various speeds, or some other type of measurement, may be needed to fully characterize pavements. The measurements that best correlate with wet-weather accidents remain to be established.

DATA ACQUISITION AND COLLATION

Traffic Volumes

Since traffic volumes vary with time, any measurement of volume not obtained at the time and location of each accident would not precisely represent the volume associated with the accident. In studies such as this that cover a system throughout a state, that type of volume measurement is highly impractical. The measurement of traffic volume that is generally available is AADT. The AADT data for 1971 were used in these analyses.

Friction Measurements

Friction measurements were obtained by using a surface dynamics pavement friction tester (model 965A) (7). This skid trailer complies with ASTM E 274 (8). The measurements represent friction developed between a standard test tire (ASTM E 249) (9) and a wetted pavement. The locked-wheel measurement is expressed as a skid number (SN); incipient or peak friction is expressed as a peak slip number (PSN).

Measurements were obtained during the summer of 1971 on all rural, four-lane, Interstate and parkway routes in Kentucky having a posted speed limit of 70 mph (31 m/s). Tests were made in the left wheel path only and at 1-mile (1.6-km) intervals in outer lanes; no less than five tests per lane were made on each construction project. The basic test speed was 70 mph (31 m/s). Additional tests were conducted on selected pavements at 40 mph (18 m/s). Comparison between the SN obtained at the two speeds is shown in Figure 1.

Accident Information

Accident data were obtained from state police records, computerized, and maintained by the Kentucky Department of Public Safety. All accidents reported during 1970, 1971, and 1972 were analyzed. A summary of accidents on rural, four-lane, Interstate and parkway routes is given in Table 1. Accidents totaled 5,907, of which 1,314 occurred during wet-surface conditions.

From these accident records, many expressions of accident occurrence may be calculated. Rates of wet-surface accidents, dry-surface accidents, fatal and injury accidents, and total accidents (including property damage accidents) are commonly calculated. Expressions used in other investigations have included the following:

1. Ratio of wet- to dry-surface accidents,
2. Ratio of wet-surface to total accidents,
3. Ratio of wet-surface, skidding accidents to total accidents,
4. Wet-surface accidents per 100 million vehicle miles (161 million vehicle km),
5. Total accidents per 100 million vehicle miles (161 million vehicle km), and
6. Fatal and injury accidents per 100 million vehicle miles (161 million vehicle km).

Test Sections

A test section is defined as a pavement section of uniform age and composition that has been subjected to essentially uniform wear along its length (8). Almost all construction projects fit this definition. Inasmuch as the direction of travel for a vehicle involved in an accident was not given in the accident reports, sections included both directions of travel. There were 110 test sections.

On rural, four-lane roadways, most traffic travels in the outer lanes (approximately 80 to 85 percent), and a large percentage of maneuvers begin or terminate there. The outer lane, left wheel path SNs were averaged to characterize the skid resistance of the test sections. Distributions of these values for the 110 test sections are shown in Figure 2 for SN and in Figure 3 for PSN. The relationship between SN and PSN is shown in Figure 4.

Mile points recorded in accident reports were used to describe the location of accidents to the nearest 0.1 mile (0.16 km). The ratios of wet- to dry-surface accidents and wet-surface to total accidents and rates of wet-surface accidents and total accidents, in terms of 100 million vehicle miles (161 million vehicle km) [total vehicle miles (kilometers) traveled under all pavement conditions], were calculated for each test section. These rates were based on the lengths of sections and the 1971 AADTs and pertain to accidents for a 3-year period. Similar calculations were made for the accident data for 6-month periods (June through November).

SKID NUMBERS AND ACCIDENTS

Analysis of Test Sections by Cross Classification

For aid in determining the relationship between combinations of traffic volume, SNs, and accidents, data for test sections were arrayed as given in Table 2. Elements of the array are average wet-surface accident rates, total accident rates, ratios of wet-surface to total accidents, and ratios of wet- to dry-surface accidents for all test sections within SN and traffic volume categories.

Analysis of the arrays led to the conclusion that the data needed to be stratified with respect to AADT to better define the relationship between accidents and pavement friction. A plot of wet-surface accident rate versus SN (Figure 5) further demonstrated the need for sorting and grouping the data. Stratification of data by AADT showed improved relationship between accidents and SNs for some accident expressions but not necessarily for other expressions. Considerable variability in data remained after

Figure 1. Correlation of 40 and 70-mph (18 and 31-m/s) trailer tests on bituminous and portland cement concrete pavements.

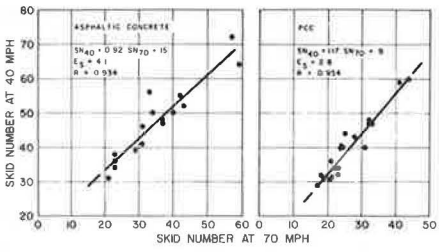

Table 1. Yearly accident occurrence on 110 test sections.

Route	Accidents				Dry-Surface Accidents				Wet-Surface Accidents				Fatalities			
	1970	1971	1972	Total	1970	1971	1972	Total	1970	1971	1972	Total	1970	1971	1972	Total
I-64	190	225	267	682	102	138	164	404	34	46	59	139	16	5	12	33
I-65	287	349	400	1,036	179	225	273	677	72	65	101	238	9	12	12	33
Kentucky Turnpike	233	222	332	787	146	168	242	556	64	29	82	175	6	5	15	14
I-71	229	254	259	742	116	132	145	393	59	66	57	184	2	6	6	70
I-75	643	597	611	1,851	395	361	361	1,117	110	140	167	417	24	29	17	26
Jackson Purchase Parkway	11	16	23	50	9	13	13	35	2	1	7	10	0	0	0	0
Pennyrile Parkway	45	51	63	159	38	38	47	123	4	3	11	18	2	3	0	5
Western Kentucky Parkway	89	76	109	274	59	51	75	185	22	15	20	57	5	3	4	12
Bluegrass Parkway	70	64	62	196	50	41	38	129	10	11	13	34	6	1	5	12
Mountain Parkway	47	32	51	130	27	19	22	68	10	11	21	42	2	2	2	6
Total	1,844	1,886	2,177	5,907	1,121	1,186	1,380	3,687	387	389	538	1,314	72	66	73	211

Figure 2. Skid number distribution for 110 test sections.

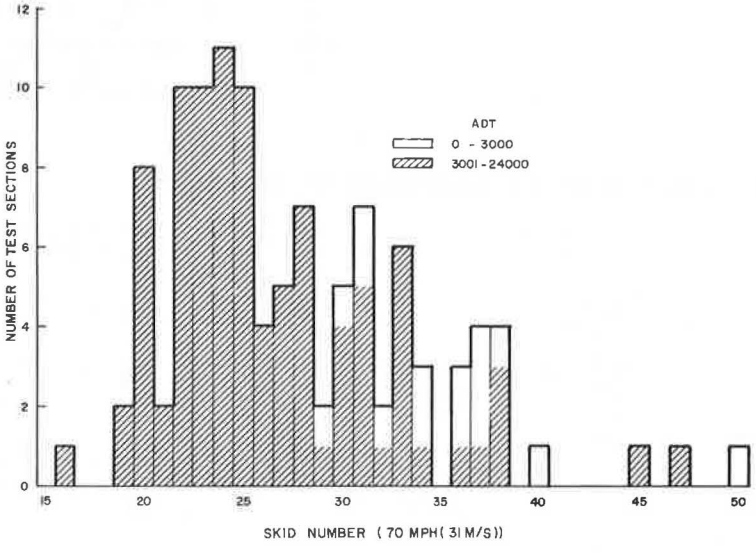

Figure 3. Peak slip number distribution for 110 test sections.

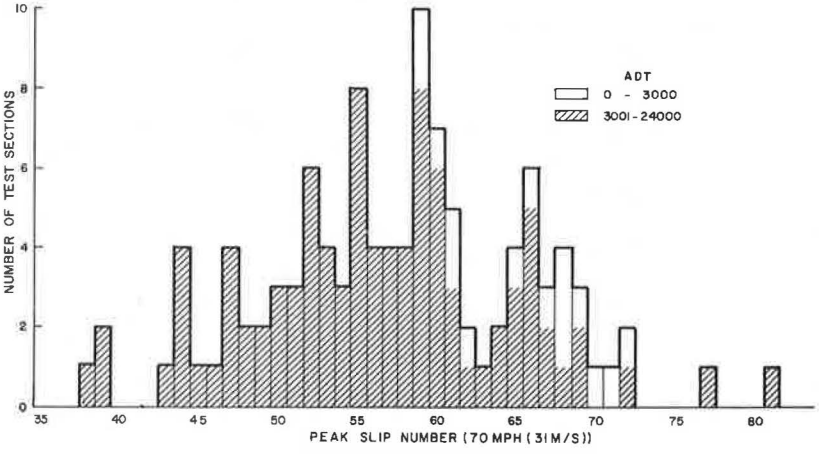

Figure 4. Relationship between skid number and peak slip number at 70 mph (31 m/s).

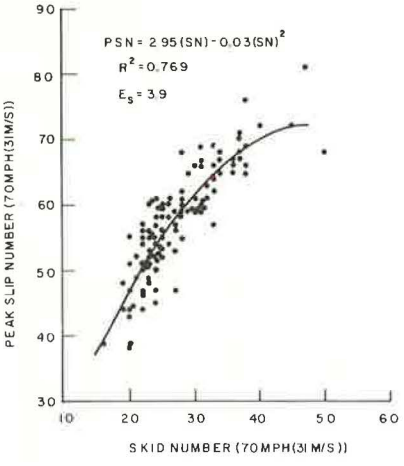

Figure 5. Test section averages for wet-surface accident rate for 1970 through 1972 versus skid number with AADT stratification.

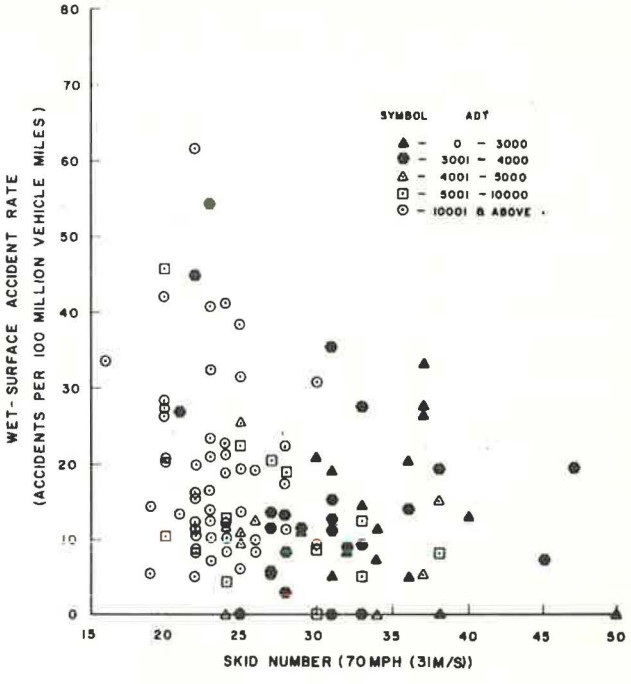

Table 2. Average accident rates at 70 mph (31 m/s) and accident ratios.

Number of Test Sections	AADT	Skid Numbers	Wet-Surface Accident Rates* 1970	1971	1972	1970 to 1972	Total Accident Rates* 1970	1971	1972	1970 to 1972	Ratio of Wet-Surface to Total Accidents 1970	1971	1972	1970 to 1972	Ratio of Wet- to Dry-Surface Accidents 1970	1971	1972	1970 to 1972
16	0 to 3,000	16 to 20																
		21 to 25																
		26 to 30	14.9	6.3	27.6	16.3	100.1	47.3	74.2	73.8	0.15	0.25	0.41	0.21	0.19	0.50	0.75	0.29
		31 to 35	15.3	8.4	9.2	11.0	51.2	82.3	61.4	65.0	0.45	0.16	0.15	0.19	0.56	0.55	0.21	0.30
		36 to 40	13.0	2.0	38.7	17.9	84.7	49.0	116.0	83.2	0.14	0.03	0.30	0.20	0.23	0.04	0.68	0.31
		41 to 50	0.0	0.0	0.0	0.0	0.0	0.0	474.4	158.1			0.0	0.0			0.0	0.0
24	3,001 to 4,000	16 to 20																
		21 to 25	24.3	27.6	42.8	31.6	113.7	78.8	109.9	100.8	0.14	0.33	0.39	0.29	0.69	0.55	1.47	1.15
		26 to 30	7.2	6.5	15.3	9.7	53.7	70.9	75.9	66.8	0.13	0.13	0.21	0.16	0.23	0.20	0.34	0.22
		31 to 35	16.1	6.2	18.1	13.5	77.0	60.3	88.2	75.2	0.15	0.10	0.18	0.16	0.33	0.24	0.32	0.27
		36 to 40	12.9	25.9	11.8	16.8	48.0	82.1	90.5	73.5	0.58	0.60	0.14	0.31	0.25	0.33	0.50	1.36
		41 to 50	22.9	5.8	11.3	13.3	82.4	76.2	64.9	74.5	0.25	0.07	0.18	0.17	0.49	0.08	0.29	0.26
19	4,001 to 9,000	16 to 20																
		21 to 25	8.0	9.1	19.4	12.2	46.6	41.9	58.1	48.9	0.18	0.24	0.35	0.24	0.40	0.52	0.90	0.45
		26 to 30	6.4	12.5	17.7	12.2	47.4	68.5	75.5	63.8	0.13	0.13	0.21	0.17	0.22	0.35	0.46	0.31
		31 to 35	11.6	0.0	6.3	6.0	58.0	31.4	82.0	57.1	0.17	0.0	0.08	0.11	0.37	0.0	0.50	0.27
		36 to 40	2.8	18.4	7.7	9.6	41.5	35.3	50.9	42.5	0.11	0.55	0.13	0.22	0.17	2.78	0.26	0.38
		41 to 50																
25	9,001 to 14,000	16 to 20	25.4	28.3	24.8	26.2	95.1	95.8	96.1	95.7	0.26	0.25	0.24	0.26	0.54	0.54	0.44	0.50
		21 to 25	16.0	13.9	20.7	16.9	66.6	86.0	91.1	81.3	0.24	0.15	0.22	0.21	0.50	0.27	0.40	0.37
		26 to 30	24.3	24.3	44.5	31.0	76.8	68.7	137.5	94.3	0.32	0.35	0.32	0.33	0.50	0.67	0.52	0.55
		31 to 35																
		36 to 40																
		41 to 50																
26	14,001 to 24,000	16 to 20	21.3	15.9	24.2	20.5	86.3	87.1	97.0	90.1	0.26	0.18	0.24	0.22	0.44	0.32	0.43	0.40
		21 to 25	18.3	20.4	26.1	21.6	87.8	85.8	104.1	92.6	0.19	0.23	0.25	0.22	0.44	0.45	0.43	0.40
		26 to 30	9.7	11.6	17.7	13.0	69.5	76.6	72.1	72.7	0.14	0.16	0.23	0.17	0.25	0.26	0.42	0.27
		31 to 35																
		36 to 40																
		41 to 50																
110	0 to 24,000	16 to 20	24.6	26.0	24.7	25.1	93.5	94.3	96.3	94.7	0.26	0.24	0.24	0.25	0.52	0.50	0.44	0.48
		21 to 25	16.1	26.7	24.5	19.1	75.2	77.0	91.6	81.3	0.20	0.21	0.27	0.23	0.48	0.41	0.61	0.47
		26 to 30	9.3	10.3	19.0	12.9	62.9	70.2	77.0	70.0	0.15	0.16	0.24	0.18	0.24	0.30	0.44	0.28
		31 to 35	15.1	5.9	13.2	11.4	65.3	62.8	78.2	68.8	0.24	0.10	0.15	0.16	0.40	0.31	0.31	0.28
		36 to 40	10.1	10.0	26.5	15.7	47.8	51.1	95.5	71.4	0.21	0.25	0.27	0.22	0.21	0.33	0.54	0.50
		41 to 50	15.3	3.9	7.5	8.9	54.9	50.0	201.4	102.4	0.25	0.07	0.12	0.11	0.49	0.08	0.19	0.18
94	3,001 to 24,000	16 to 20	24.6	26.0	24.7	25.1	93.5	94.3	96.3	94.7	0.26	0.24	0.24	0.25	0.52	0.50	0.44	0.48
		21 to 25	16.1	16.7	24.5	19.1	75.2	77.0	91.6	81.3	0.20	0.21	0.27	0.23	0.48	0.41	0.61	0.47
		26 to 30	8.8	10.7	18.2	12.6	59.3	72.4	77.3	69.7	0.15	0.15	0.22	0.18	0.25	0.28	0.41	0.27
		31 to 35	14.9	4.6	15.2	11.6	72.3	53.1	86.6	70.7	0.15	0.07	0.16	0.15	0.34	0.18	0.37	0.27
		36 to 40	6.8	21.4	9.4	12.5	44.1	54.0	66.7	54.9	0.30	0.57	0.14	0.26	0.19	2.16	0.35	0.78
		41 to 50	22.9	5.8	11.3	13.3	82.4	76.2	64.9	74.5	0.25	0.07	0.18	0.17	0.49	0.08	0.29	0.26

*Per 100 million vehicle miles (161 million vehicle km).

elimination of test sections having AADTs less than 3,000 vehicles per day. However, a trend was unmistakable: Wet-surface accident rates decreased as SNs increased. Resulting relationships between accidents and pavement friction involving the wet-surface accident rate are shown in Figure 6 and for other accident expressions in Figures 7, 8, and 9. (Data in Figures 6 through 18 are stratified at an AADT of 3,000 per day.)

Analysis of data for test sections with AADTs above 3,000 continued so that the expression of accident occurrence relating best to pavement friction could be found. This was accomplished by taking elements in the arrays as predicted values. Actual accident occurrences for each test section were then compared to this predicted value to obtain deviations. This enabled computation of a coefficient of correlation for each accident expression. The correlation coefficients ranked the expressions in the following order:

1. Wet-surface accidents per 100 million vehicle miles (161 million vehicle km),
2. Total accidents per 100 million vehicle miles (161 million vehicle km),
3. Ratio of wet-surface to total accidents, and
4. Ratio of wet- to dry-surface accidents.

The degree of correlation was not sufficiently encouraging to enable a decisive selection of the best expression. Therefore, all four expressions were used in further analyses to determine the relationship between accident occurrence and pavement friction.

Analysis of Test Sections by Averaging Techniques

Three averaging methods were used to reduce variability and, thereby, to more clearly demonstrate general relationships already apparent in the data set for test sections having AADTs above 3,000 vehicles per day. A discussion of these methods and the resulting trends follows.

Cumulative Averages

In the first method, two techniques were used to calculate cumulative averages. The first involved calculating the average of each expression for accident occurrence for all test sections having an SN less than or equal to a given value. The second procedure involved calculating average accident occurrence, for each method of expression, of all test sections having an SN greater than a given value. These average values are plotted as shown in Figures 10, 11, 12, and 13.

In the first procedure of calculating averages, accident occurrences for low SNs had greater influence on the average value obtained. Extreme values of the expressions for accident occurrence for a test section at high SNs were attenuated through division by the large number of test sections with lower SNs. Thus, the second procedure, which yielded opposite weightings, was necessary to verify the trends and to ensure that large deviations at high SNs were not being masked by the averaging process. The resulting trends were reasonably similar for wet-surface and total accident rates. For other expressions, the trend lines were not so similar, and the data points were quite scattered. Wet-surface accident rate decreased as SNs increased to approximately 28; further increase in SNs resulted in only slight reduction in accidents. Since the trends were similar and because of the ranking of accident expressions discussed previously, subsequent analyses were restricted to using wet-surface accidents per 100 million vehicle miles (161 million vehicle km) as the method of expressing accident occurrences.

Average Wet-Surface Accident Rates Grouped by Skid Number

In the second method, test sections were grouped by SNs. The average wet-surface accident rate was calculated for each group; these averages are plotted as shown in

Figure 6. Wet-surface accident rate versus skid number.

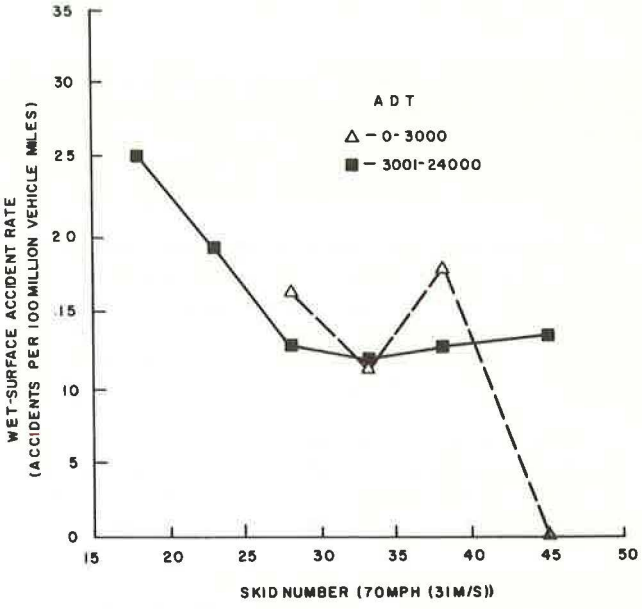

Figure 7. Total accident rate versus skid number.

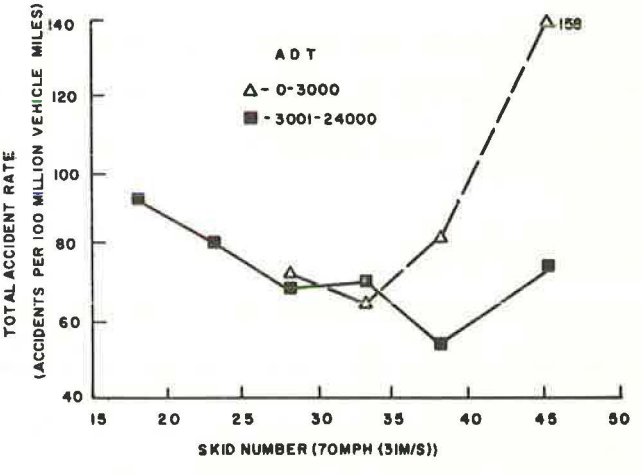

Figure 8. Ratio of wet-surface to total accidents versus skid number.

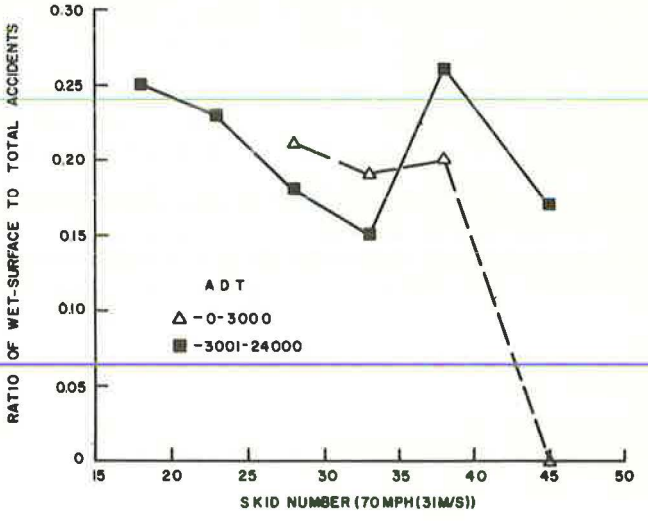

Figure 9. Ratio of wet- to dry-surface accidents versus skid number.

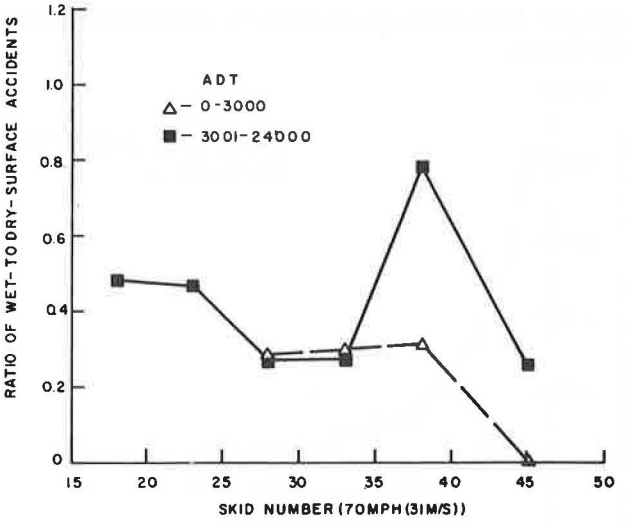

Figure 10. Average wet-surface accident rate versus skid number.

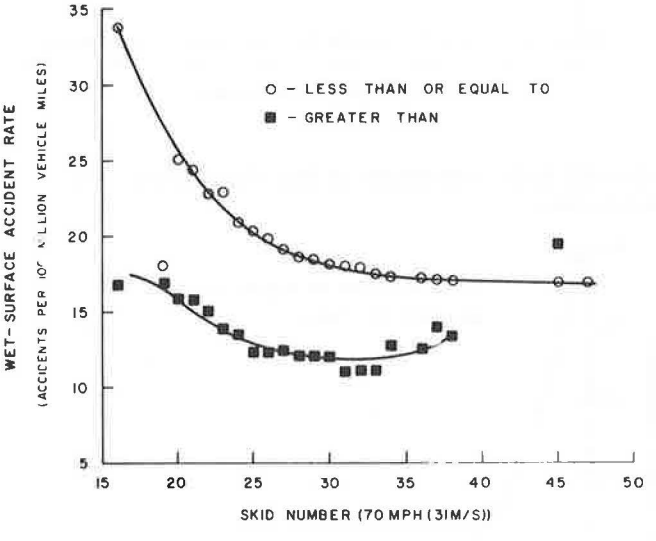

Figure 11. Average total accident rate versus skid number.

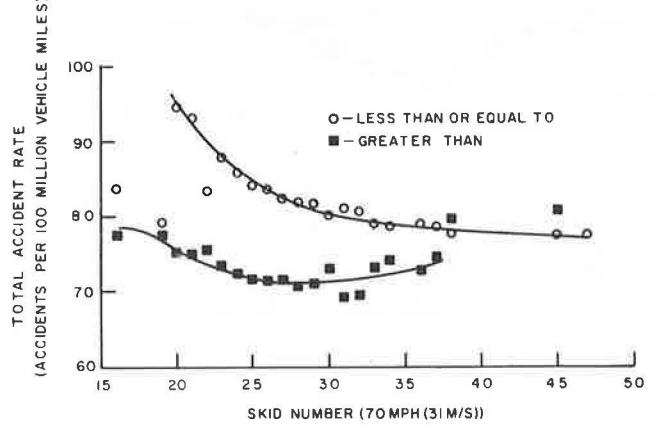

Figure 12. Ratio of average wet-surface to total accidents versus skid number.

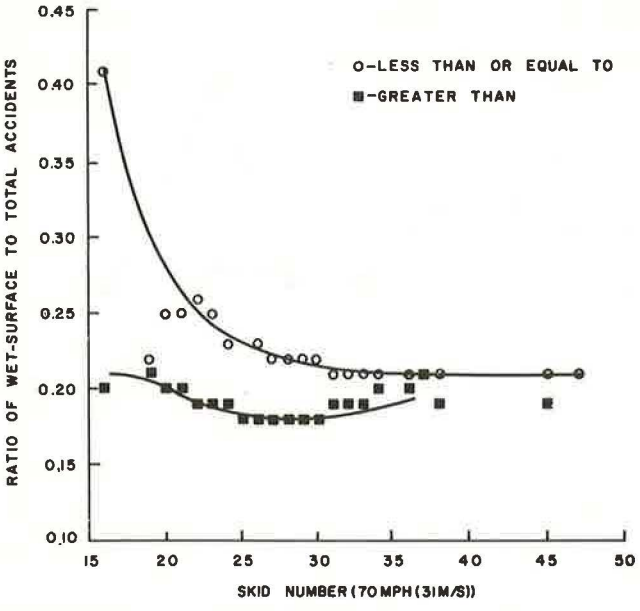

Figure 13. Ratio of average wet- to dry-surface accidents versus skid number.

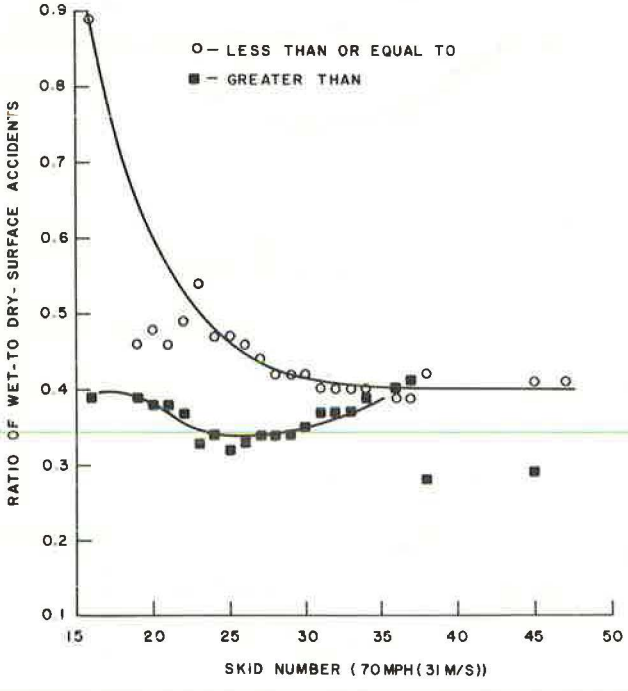

Figure 14. Again the trend indicated that accident rate rapidly decreased as SNs increased SNs up to about 27. The variability was greater than that obtained by the first method because several groups included only one or two test sections, each having equal weighting as groups containing a larger number of test sections. Still, the trends indicated by the two methods were quite similar.

Moving Averages

The third method involved calculation of an average wet-surface accident rate and an average SN for progressively ordered sets of five test sections. The first average was of the five test sections with the lowest SNs. The test section with the lowest SN was then dropped, and a test section with the next highest SN was added. This was repeated until all test sections had been averaged in a group of five. In cases where more than one test section had the next highest SN, one of these was randomly added each time. Test sections were dropped in the same sequence as they were added. Resulting averages are plotted as shown in Figure 15.

The trend was similar to those developed by the previous two methods; however, moving averages indicated a more distinct change in the slopes of the two branches of the curve. At SN < 27, the wet-surface accident rate increased by two to three accidents per 100 million vehicle miles (161 million vehicle km) per SN; at SN > 27, the wet-surface accident rate decreased nominally.

The foregoing analysis involved accident data for the entire 3 years while skid resistance was measured in the summer and fall of 1971. Pavements, of course, exhibit lower friction in the summer and fall, but the measured values may not be assumed to necessarily represent the lowest friction during the year for a particular pavement nor for the road system as a whole. The rapid change in the slope of the curve in Figure 15, for instance, may occur at some higher or lower SN depending on when measurements are made. If accident data were subdivided into subsets for two periods of the year and the measured values reflected the mean SN for each period, the rapid change in the slope would then be expected to occur at the same SN, provided driver behavior remained the same throughout the year. Since skid-resistance values were not available for the winter-spring period, Figure 16 was prepared to show the relationship between wet-surface accident rate and pavement friction for the summer-fall period. In contrast to Figure 15, a slightly higher SN at which the accident rate increased rapidly is evident. The data, however, are more scattered, presumably because of the reduced data base. A shift toward a higher SN would be anticipated because the accident rates associated with the 3-year period were related to friction values that were lower than the mean friction for a full year. Because of greater scatter of data in Figure 16, the trend established in Figure 15 must be accepted as the better indication of the relationship between accidents and pavement friction, even though the accident data in Figure 16 more closely correspond to the measured skid resistance.

Wet-surface accident rates were calculated for 100 million miles (161 million km) of total travel under all pavement conditions rather than for only wet-surface travel. The true accident rate for wet-surface conditions would be several times higher since pavements were wet only 13 percent of the time. In addition, as given in Table 3, precipitation from June to November was substantially less than from December to May. Yet, the wet-surface accident rates for 1970 and 1971 were higher during the period from June to November. Precipitation in 1972, especially during the winter-spring period, was substantially more than that in the two preceding years. If precipitation for the two 6-month periods (during 3 years) were the same, the wet-surface accident rate of 19.5 (June to November) would be 25.2 compared with 19.3 for winter-spring periods. Therefore, lower skid resistance of pavements during summer and fall obviously contributed to an increase in wet-surface accidents.

PEAK SLIP NUMBERS AND ACCIDENTS

As discussed previously, there is a need to analyze different measurements of pavement

Figure 14. Average wet-surface accident rate of 94 test sections grouped by skid number versus skid number.

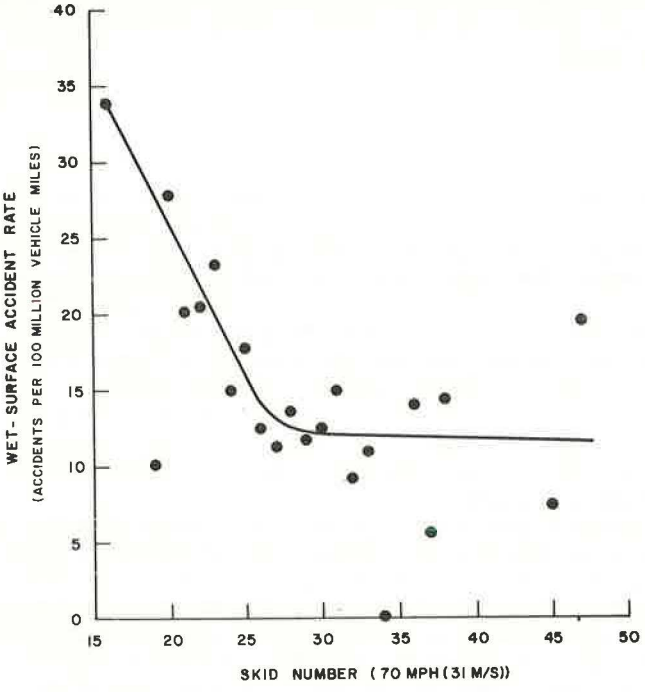

Figure 15. Five-point moving averages for wet-surface accident rate versus skid number.

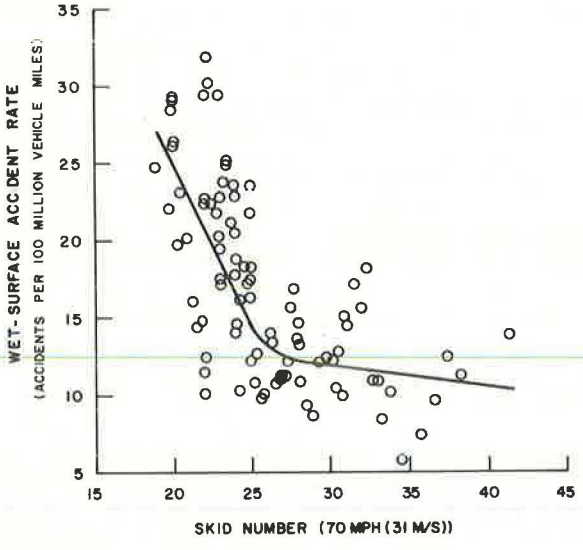

Figure 16. Five-point moving averages for wet-surface accident rate for summer-fall period versus skid number.

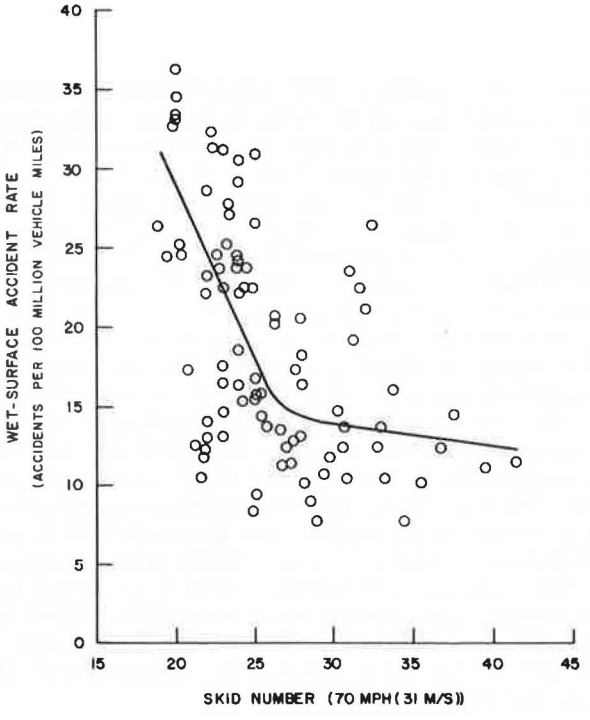

Table 3. Semiannual accident data.

Year	Period	Number of Accidents			Ratio of Accidents		Accident Rates[a]			Precipitation[b] (percent)
		Total	Dry-Surface	Wet-Surface	Wet to Total	Wet to Dry	Total	Dry	Wet	
1970	December to May	965	476	166	0.17	0.35	92.3	45.6	15.9	13
	June to November	879	645	221	0.25	0.34	66.9	49.1	16.8	10
1971	December to May	948	511	160	0.17	0.31	90.7	48.9	15.3	13
	June to November	938	676	229	0.24	0.34	71.4	51.5	17.4	10
1972	December to May	1,029	542	280	0.27	0.52	98.5	51.9	26.8	18
	June to November	1,148	838	278	0.24	0.33	87.4	63.8	21.2	12
1970 to 1972	December to May	2,942	1,529	606	0.21	0.40	93.8	48.8	19.3	15
	June to November	2,965	2,159	728	0.25	0.34	75.3	54.8	18.5	11

[a]Per 100 million vehicle miles (161 million vehicle km) for all pavement conditions.
[b]Trace or more in the Lexington area; periods of snow or ice not included.

Figure 17. Average wet-surface accident rate of 94 test sections grouped by peak slip number versus peak slip number.

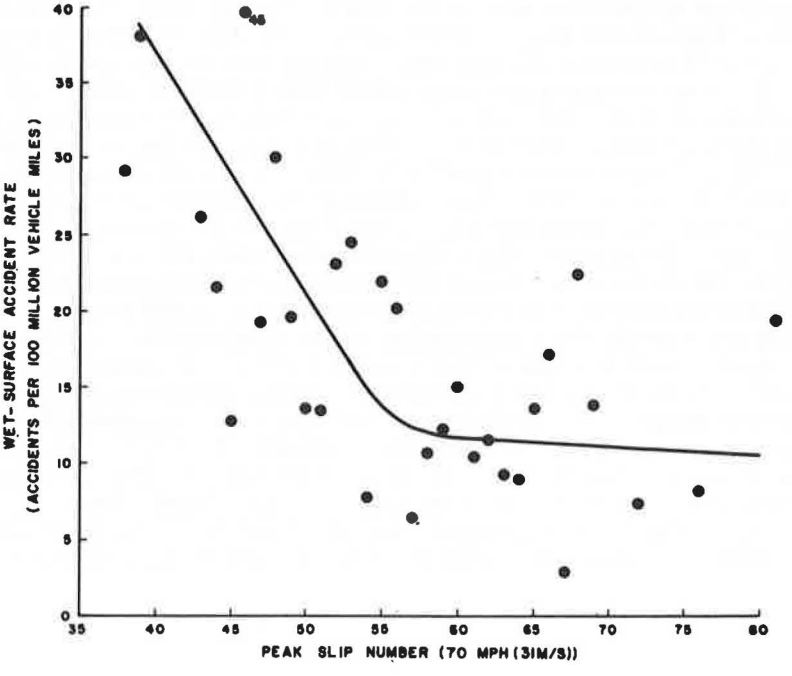

friction to determine which correlates best with accident experience. The peak friction force was measured routinely during all tests; thus these data were available for analysis. Test section averages were arrayed as given previously, but PSNs were substituted for SNs. The arrays again indicated the desirability for sorting the data by AADT at 3,000 vehicles per day. Wet-surface accident rates again appeared to be the best expression for accident occurrence. Test sections were grouped by PSN, and average wet-surface accident rates were calculated for each PSN as shown in Figure 17, which indicates more scatter than was obtained with SNs (Figure 14); this may be because each data point represents fewer test sections. The greatest change of slope occurred at PSN $\approx$ 57. Similar results were obtained by using five-point moving average, as shown in Figure 18, and the change in slope remained at the same PSN.

The point of greatest change in slope of the curve in Figure 18 was at PSN = 57 and in Figure 15 at SN = 27. According to Figure 4, a PSN of 57 is equivalent to SN of approximately 27. Scatter of the data in Figure 15 and Figure 18 also appears to be similar and, therefore, suggests that both measurements of friction related equally well to accident occurrence. This was somewhat unexpected because of the inherent measurement and chart analysis errors associated with determination of peak slip resistance (PSN). Peak slip resistance occurs for a very brief period of time during wheel lock-up, and measurement represents a much shorter length of pavement than the locked-wheel test (SN). For that reason, poor agreement between SN and PSN in Figure 4 was credited largely to inaccuracies in PSN. If such a conclusion is valid, some of the scatter of data in Figure 18 may be due to errors in PSN. In that event, PSN may correlate best with accident experience.

SUMMARY AND CONCLUSIONS

On rural, four-lane, Interstate and parkway (expressway) facilities, wet-surface accidents per 100 million vehicle miles (161 million vehicle km) correlated best with skid resistance. Even when the best statistical expression of accidents is used, scatter and spurious variability in data seem inevitable. Stratification of the data by AADT at 3,000 vehicles per day minimized scatter. Averaging methods as a means of developing trends and minimizing scatter between variables were used in the study. Of the averaging methods investigated, the moving average yielded more definitive results. Definite trends were established in regard to the relationship between wet-surface accident rates and SNs (Figure 15). Wet-surface accident rate [at 70 mph (31 m/s)] decreased rapidly as the SN increased to 27; further increases in SN beyond this point resulted in only a slight reduction in accident rate. The analysis involved accident data throughout the year (3-year period), and skid resistances were measured in the summer and fall (1971) when pavements normally exhibit lower friction values. As expected, analysis of the accident data for June to November (Figure 16) indicated a slightly higher friction. The data, however, were more scattered because of the reduced data base.

Wet-surface accident rates for 2 of the 3 years considered in this study were higher during the summer-fall periods (Table 3) even though the roads were wet a lesser proportion of time. When adjusted to equal time of precipitation during December to May and June to November, wet-surface accident rates for the summer-fall periods were higher for all 3 years. Lower skid resistance of pavements during summer and fall obviously contributed to an increase in wet-surface accidents.

Definite trends were also evident between wet-surface accident rates and PSNs. The greatest change in slope of the trend lines (Figure 16) occurred at a $PSN_{70} \approx 57$. Scatter of data was no worse than that for SNs. This was somewhat unexpected because of the inherent measurement and chart analysis errors associated with determination of peak slip resistance. PSN = 57 is equivalent to SN $\approx$ 27 (Figure 15); SN_{70} = 27 also corresponds to the greatest change in slope of trend lines. This suggests either that the correlation between the two friction measurements overshadowed any subtle differences that may exist between accidents and either measurement of friction or that both skid and slip resistance are equally valid indexes of friction requirements for pavements.

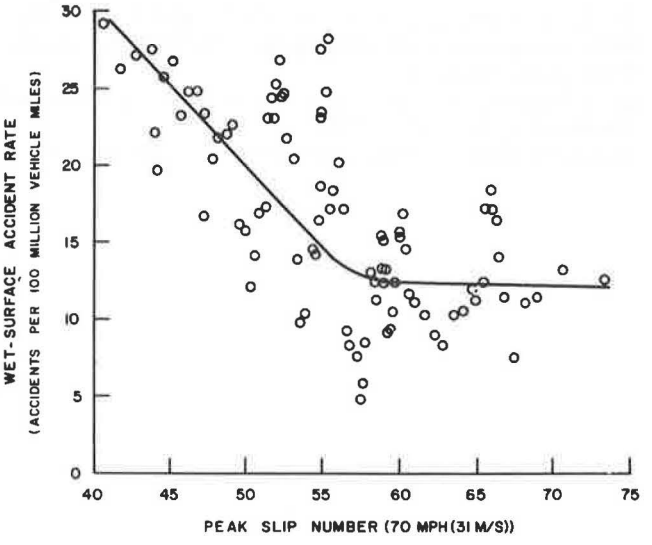

Figure 18. Five-point moving averages for wet-surface accident rate versus peak slip number.

It should be reemphasized that the findings in this paper pertain to rural, four-lane, limited-access, expressway types of highways with posted speeds of 70 mph (31 m/s) and that no consideration was given in the analysis to geometrics of roadways or to points of traffic conflicts. High accident or repeat-accident locations certainly warrant further study to determine what variables or combination of variables may contribute to wet-surface accidents. Nevertheless, it was demonstrated that there is a relationship between accident experience and pavement friction; this relationship should be used as a guide in establishing minimum friction requirements for pavements. The established trends, relating wet-surface accident rates with skid resistance, indicated a definite value of skid resistance below which the accident rate increased rapidly. In addition, the methods described may be used in future analyses to establish skid-resistance requirements for other types of highways.

ACKNOWLEDGMENTS

The work reported in this paper was done by the Bureau of Highways, Kentucky Department of Transportation, in cooperation with the Federal Highway Administration. Contents of the paper reflect the views of the authors and not necessarily the official views or policies of the Bureau of Highways or FHWA.

REFERENCES

1. C. G. Giles. The Skidding Resistance of Roads and the Requirements of Modern Traffic. Proc., Institution of Civil Engineers, Vol. 6, Feb. 1957.
2. B. E. Sabey. Road Surface Characteristics and Skidding Resistance. Journal of British Granite and Whintone Federation, Vol. 5, No. 2, Autumn 1965.
3. B. F. McCullough and K. D. Hankins. Skid Resistance Guidelines for Surface Improvements on Texas Highways. Highway Research Record 131, 1966, pp. 204-217.
4. H. W. Kummer and W. E. Meyer. Tentative Skid Resistance Requirements for Main Rural Highways. NCHRP Rept. 37, 1967.
5. D. C. Mahone and S. N. Runkle. Pavement Friction Needs. Highway Research Record 396, 1972, pp. 1-12.
6. A. B. Moore and J. B. Humphreys. A Study of Pavement Skid Resistance at High Speed and at Locations Shown to be Focal Points of Accidents. Department of Civil Engineering, University of Tennessee, April 1972.

7. R. L. Rizenbergs, J. L. Burchett, and C. T. Napier. Skid Test Trailer: Description, Evaluation and Adaptation. Division of Research, Kentucky Department of Highways, Sept. 1972.
8. Skid Resistance of Paved Surfaces Using a Full-Scale Tire, E 274-70. Annual ASTM Standards, Part 11, 1973.
9. Standard Tire for Pavement Tests, E 249-66. Annual ASTM Standards, Part 11, 1973.

ANALYSIS OF ROAD PROFILES BY USE OF DIGITAL FILTERING

Hugh J. Williamson, Center for Highway Research, University of Texas at Austin

This paper discusses the use of digital filtering to analyze measured road profiles. Applications of road roughness analysis are given. The discussion of the signal processing operators emphasizes considerations, including pitfalls, that are particularly important. The purpose of filtering is to isolate, for further analysis, the roughness of a given type, e.g., that with 10 to 30-ft (3 to 9-m) wavelengths. Such analysis might include the calculation of measures of overall or average roughness and the most severe roughness in a road section. Both artificial and real test cases are given to compare and demonstrate the capabilities of selected filters. A particular type of filter is recommended on the basis of the test cases. Digital filter design by specification of the squared-magnitude function is emphasized. Selected results from a pilot study in which comparisons are made between hot-mixed asphalt concrete and surface-treated pavements are given to demonstrate the application of the suggested filter and roughness measures.

•A DEVICE such as the surface dynamics (SD) profilometer can be used to measure a road profile, i.e., surface elevation versus distance along the road in both the right and left wheel paths (7, 8, 9). The road profiles themselves characterize the road roughness in that they contain information from which one can infer the nature and extent of the roughness.

Although plotted profiles are convenient for visual inspection and comparison of roads, other direct uses of measured profiles are limited because of the very large amount of data required to describe a road surface. Further use of the data is greatly facilitated by the calculation of a set of summary roughness measures. Such mathematical analyses as development of a regression model to predict serviceability (human panel evaluations of riding quality) in terms of pavement roughness require summary measures (5, 9, 10). The set should be small in number and be meaningful physically, e.g., from the standpoint of riding quality.

In this paper, road roughness is characterized based on the right and left profiles measured by an instrument such as the SD profilometer. The techniques to be discussed are by no means limited to analysis of the data from a particular measuring system; it is anticipated that they will be used in the future in conjunction with new systems, such as the noncontacting probe now being developed under contract to the federal government.

The potential for application of roughness analysis is great. Although it is not feasible to discuss all possibilities, for the purpose of illustration, new pavement evaluation, pavement feedback, study of effects of maintenance, and analyses of road user satisfaction are discussed as follows:

1. Roughness analysis based on measurements by the SD profilometer would be useful in evaluating new pavements. A future application might be the design of a set of acceptance criteria, including minimally acceptable levels of various classes of roughness, for new pavements. The decomposition of roughness into classes is discussed later in the paper.
2. Sophisticated roughness evaluation could be used for field evaluation of the roughness characteristics of different kinds of pavements. A comparison of roughness com-

ponents of bridges and nearby pavement and analysis of the short-wavelength roughness found near the ends of bridges would also be valuable, and comparisons could be made between the roughness components of samples of new and deteriorated pavements of a given type. The insights gained about predominant classes of roughness and roughness growth patterns in different kinds of pavements would be useful in evaluating construction practices.

3. Roughness analysis would allow quantitative comparisons between pavements immediately before and after maintenance. The objectives of this analysis include (a) determining whether a given type of maintenance is adequate and whether there are types of roughness the maintenance does not correct and (b) comparing different types of maintenance on the basis of improvement of different classes of roughness.

If the objective of the maintenance were to repair a few severely distressed places in a road section, overall roughness measures, such as a power spectrum, would not be adequate. Measures indicating the severity of the worst roughness in the section would be required. Because the power spectrum is not of central importance here, it will not be discussed in detail. Spectral analysis can be thought of as a method for computing a roughness measure for each of a finite set of wavelengths. Power spectra are discussed elsewhere (2, 8, 9, 10). Follow-up analyses at intervals of, say, 6 months would be useful in assessing the continuing effect of maintenance.

4. A study in which a regression model was developed to predict pavement serviceability in terms of power spectra of road profiles is discussed elsewhere (9, 10). In human-panel serviceability ratings, the fact that 89 percent of the road-to-road variation was explained in terms of the roughness measures (9, p. 25) proves that there is a close relationship between a human's evaluation of a road and roughness measures obtainable by signal processing of the road profile. Further work in this area could include a study of the relationships between serviceability and the individual components of roughness to determine which aspects people find most objectionable. This research would have application in the three areas previously discussed.

OBJECTIVES

Decomposition of the profile roughness on a frequency basis has been investigated and, as stated above, has been shown to be useful in explaining human-panel serviceability ratings. Although the power spectrum approach is effective and computationally efficient for computing overall roughness measures, digital filtering methods can be used to isolate the roughness within each of an arbitrary set of wavelength bands, and, subsequently, measures of local roughness, such as local root-mean-square (rms) amplitudes at a discrete set of points within the section, can be computed for each band. Thus, measures of overall roughness and of extreme roughness within the section can be computed.

Digital filtering here refers simply to the formation of a new road profile, y_i, $i = 1, \ldots, N$, from an input profile, x_i, $i = 1, \ldots, N$, by an operation such as

$$y_n = \sum_{i=0}^{r} K_i x_{n-i} - \sum_{i=1}^{s} L_i y_{n-i} \qquad (1)$$

The convention $x_i = y_i = 0$ for $i < 0$ can be adopted to allow calculation of the first few points. The coefficients K_i and L_i are chosen according to the purpose to be achieved, e.g., to produce a profile y_i with all roughness removed except that with 10 to 30-ft (3 to 9-m) wavelengths. The passband is the band of frequencies or wavelengths of the information to be isolated. In this example, the passband is 10 to 30-ft (3 to 9-m) wavelengths or, equivalently, $^1/_{30}$ to $^1/_{10}$-cycle/ft (0.109 to 0.328-cycle/m) frequencies. A hypothetical sinusoid with a 10-ft (3-m) wavelength goes through one full cycle in 10 ft (3 m); thus, each foot (0.3 m) contains $^1/_{10}$ of a cycle, and the frequency is therefore

1/10 cycle/ft (0.328 cycle/m). Actually the cutoff at the edges of the passband is imperfect; some waves near the edges of the band, both within and without, are present in the filtered output at reduced amplitudes. The phrase sharpness of cutoff is used henceforth to refer to the extent of this phenomenon.

Plots of filtered and unfiltered road profiles are presented later in the paper to illustrate the isolation of roughness with wavelengths within a given band. A filter is called low pass, high pass, or band pass if, respectively, waves with low, high, or band-limited frequencies are to be isolated.

Since the profile in either wheel path is simply the surface elevation versus distance along the road, their pointwise difference is the elevation of one wheel path relative to the other versus distance. Changing elevations in one wheel path relative to the other cause vehicle roll, and are, therefore, related to ride quality. The analysis discussed above can be applied to the pointwise-difference profile to study transverse roughness.

Note that a difference in the vertical reference levels for the right and left profiles would introduce a spurious zero-frequency component into the difference profile (2). Similarly, a zero frequency component would be present if the pavement were sloped for drainage purposes; however, this is of no concern, since the zero-frequency component, which is not interpretable as roughness, would be removed by filtering.

PITFALLS

Caution must be used in selecting a digital filtering method. The following pitfalls must be kept in mind:

1. Digital filters tend to smooth the amplitudes of the input profiles over several 1/2 cycles. If an extremely narrow-band filter with sharp cutoff characteristics were used, the smoothing might be so great that the cycle-to-cycle amplitude variations in the filtered output, which are of interest, could become less than measurement error. If this were the case, calculation of the distribution of roughness within a section would clearly be futile.
2. Filters introduce phase shifts that vary with frequency, thus distorting the profile. A phase shift can be thought of as a spatial translation. Thus, a frequency-dependent phase shift translates surface deformations of different wavelengths relative to each other. An approach such as presented elsewhere (6, p. 41) can be used to eliminate this problem. If the profile is filtered forward and then the output profile is filtered backward, the phase shifts of the two operations cancel, thus yielding a filtered output free of phase shift. The forward filter should be extended beyond the data record to allow transients to die out. The double filter has sharper cutoff characteristics but produces somewhat more amplitude-smoothing distortion than a single filter. The double filter was used in all test cases discussed in this paper.
3. Road profiles are known generally to have amplitudes that increase sharply as wavelength increases. Thus, if the roughness in a band of wavelengths (λ_l, λ_u) is to be isolated, there must be a reasonably sharp cutoff at the long-wavelength edge of the passband to avoid overshadowing of the roughness within the passband by longer waves.
4. Some attention must be paid to the filter end effects at the first and last of the data record. If zeroes are extended beyond the data (to allow calculation of the first few points in both the forward and backward filtering operations), then the profile is discontinuous at the endpoints. If the terminal ordinates are extended, then the first derivatives are discontinuous at the endpoints. In either case, spurious waves are introduced near the endpoints by the filter.

The simplest solution is to exclude a short interval at the beginning and end of the record after filtering. For the filters for which test cases are presented in this paper, one cycle of the longest wave in the passband of interest has been found to be adequate. Alternatively, a nonlinear extension, chosen to be continuous at the endpoints and decay to zero within a reasonably short distance beyond the endpoints, could be used. Of course, the frequency composition of the extension should be considered relative to that near the end of the data record. The end effects may be unimportant if only overall

rms values are calculated but can have significant effects in the upper tail of the distribution of local rms values.

CHOICE OF FILTER

The low-pass digital filter specified by the squared gain is as follows:

$$G^2(\omega) = \frac{1}{1 + [\tan^{2n}(\omega T/2)/\tan^{2n}(\omega_c T/2)]} \tag{2}$$

where

$G(\omega)$ = gain at frequency ω;
ω = frequency in radians per unit change in the independent variable, wavelength = $2\pi/\omega$;
T = step size of the independent variable; and
ω_c = cutoff frequency.

Equation 2 has been found to be very effective. The gain $G(\omega)$ can be thought of as the fraction of the amplitude of a steady sinusoid of a given frequency retained after the filtering process. Ideally, the gain would be unity in the passband and zero elsewhere; realistically, we know that a rectangular gain versus frequency function can only be approximated.

As the integer n, referred to as the order of the filter, increases, the sharpness of the cutoff and the number of terms required both increase; in equation 1, r = s = n. The system output for the squared-gain function for the low-pass filter is shown in Figure 1, and plots of these filters are shown in Figure 2. The phase shift of the filter is not shown, since, as is discussed in the preceding section, the shift can be eliminated by a double-filtering operation.

It is possible to design a filter of any order of this type with any positive value of ω_c less than the Nyquist frequency of π/T radians. Thus, for example, if one wanted to look at the part of the road roughness with wavelengths of 10 ft (3 m) or more, one would select 10 ft = 2π radians/ω_c or $\omega_c = 2\pi/10$ radians/ft = $\frac{1}{10}$ cycle/ft (0.328 cycle/m). When ω_c is chosen, the coefficients (K_i and L_i in equation 1) required for using the filter can be derived. The derivation from equation 2 of the coefficients is lengthy. Thus, to allow further discussion of ride quality applications, we recommend another source (4) for the mathematical background, which will not be repeated here.

It was computationally efficient to use differences between low-pass filtered outputs to isolate the irregularities in a contiguous set of passbands. This is verified by comparing the number of filtering operations and the number of terms per filter of either the low-pass or band-pass type to achieve the same objective.

The following are considered to be desirable characteristics of the tangent form of the squared-magnitude-specified filter:

1. Having relatively sharp cutoff for a given order (i.e., a relatively low order is required to achieve a given frequency resolution) and being recursive, the filter is computationally efficient. A filter is recursive if at least one y term is included in the sum on the right of equation 1. Thus, a recursive filter uses previously computed filtered values in subsequent filtering operations. Recursive filters are generally more efficient than nonrecursive filters.
2. Gain versus frequency function is monotone; there are no spurious ripples, as with the Chebyshev filter, a well-known filter mentioned here only for comparison.
3. Flat-topped gain versus frequency function (Figure 1), as contrasted to that of, say, the curve-topped digital resonator, yields results that are somewhat more easily interpreted physically.

Figure 1. System output for squared-gain function for low-pass filter.

FREQUENCY (cy./ft.)	WAVELENGTH (ft.)	ORDER 2	ORDER 4	ORDER 6	ORDER 8	ORDER 10
0.	---	1.00000E+00	1.00000E+00	1.00000E+00	1.00000E+00	1.00000E+00
5.00000E-03	2.00000E+02	9.99994E-01	1.00000E+00	1.00000E+00	1.00000E+00	1.00000E+00
1.00000E-02	1.00000E+02	9.99906E-01	1.00000E+00	1.00000E+00	1.00000E+00	1.00000E+00
1.50000E-02	6.66667E+01	9.99496E-01	1.00000E+00	1.00000E+00	1.00000E+00	1.00000E+00
2.00000E-02	5.00000E+01	9.98408E-01	9.99997E-01	1.00000E+00	1.00000E+00	1.00000E+00
2.50000E-02	4.00000E+01	9.96122E-01	9.99985E-01	1.00000E+00	1.00000E+00	1.00000E+00
3.00000E-02	3.33333E+01	9.91992E-01	9.99935E-01	9.99999E-01	1.00000E+00	1.00000E+00
3.50000E-02	2.85714E+01	9.85262E-01	9.99776E-01	9.99997E-01	1.00000E+00	1.00000E+00
4.00000E-02	2.50000E+01	9.75114E-01	9.99349E-01	9.99983E-01	1.00000E+00	1.00000E+00
4.50000E-02	2.22222E+01	9.60719E-01	9.98331E-01	9.99932E-01	9.99997E-01	1.00000E+00
5.00000E-02	2.00000E+01	9.41328E-01	9.96130E-01	9.99758E-01	9.99985E-01	9.99999E-01
5.50000E-02	1.81818E+01	9.16361E-01	9.91738E-01	9.99240E-01	9.99931E-01	9.99994E-01
6.00000E-02	1.66667E+01	8.85507E-01	9.83557E-01	9.97843E-01	9.99721E-01	9.99964E-01
6.50000E-02	1.53846E+01	8.48803E-01	9.69246E-01	9.94380E-01	9.98994E-01	9.99821E-01
7.00000E-02	1.42857E+01	8.06678E-01	9.45686E-01	9.86423E-01	9.96712E-01	9.99210E-01
7.50000E-02	1.33333E+01	7.59936E-01	9.09262E-01	9.69439E-01	9.90140E-01	9.96864E-01
8.00000E-02	1.25000E+01	7.09693E-01	8.56655E-01	9.35937E-01	9.72763E-01	9.88676E-01
8.50000E-02	1.17647E+01	6.57256E-01	7.86202E-01	8.75803E-01	9.31142E-01	9.62869E-01
9.00000E-02	1.11111E+01	6.03995E-01	6.99365E-01	7.80128E-01	8.44033E-01	8.91938E-01
9.50000E-02	1.05263E+01	5.51202E-01	6.01342E-01	6.49443E-01	6.94686E-01	7.36460E-01
1.00000E-01	1.00000E+01	5.00000E-01	5.00000E-01	5.00000E-01	5.00000E-01	5.00000E-01
1.05000E-01	9.52381E+00	4.51271E-01	4.03459E-01	3.57414E-01	3.13858E-01	2.73353E-01
1.10000E-01	9.09091E+00	4.05642E-01	3.17774E-01	2.41215E-01	1.78281E-01	1.28976E-01
1.15000E-01	8.69565E+00	3.63495E-01	2.45927E-01	1.57005E-01	9.61361E-02	5.72625E-02
1.20000E-01	8.33333E+00	3.24998E-01	1.88193E-01	1.00409E-01	5.09997E-02	2.52222E-02
1.25000E-01	8.00000E+00	2.90155E-01	1.43163E-01	6.39300E-02	2.71584E-02	1.12824E-02
1.30000E-01	7.69231E+00	2.58844E-01	1.08712E-01	4.08574E-02	1.46590E-02	5.16887E-03
1.35000E-01	7.40741E+00	2.30866E-01	8.26510E-02	2.63319E-02	8.05223E-03	2.43068E-03
1.40000E-01	7.14286E+00	2.05968E-01	6.30436E-02	1.71541E-02	4.50694E-03	1.17299E-03
1.45000E-01	6.89655E+00	1.83878E-01	4.83107E-02	1.13079E-02	2.57027E-03	5.80255E-04
1.50000E-01	6.66667E+00	1.64319E-01	3.72236E-02	7.54484E-03	1.49258E-03	2.93836E-04

Figure 2. Squared gains of filters specified by tangent form of squared-magnitude approximating function.

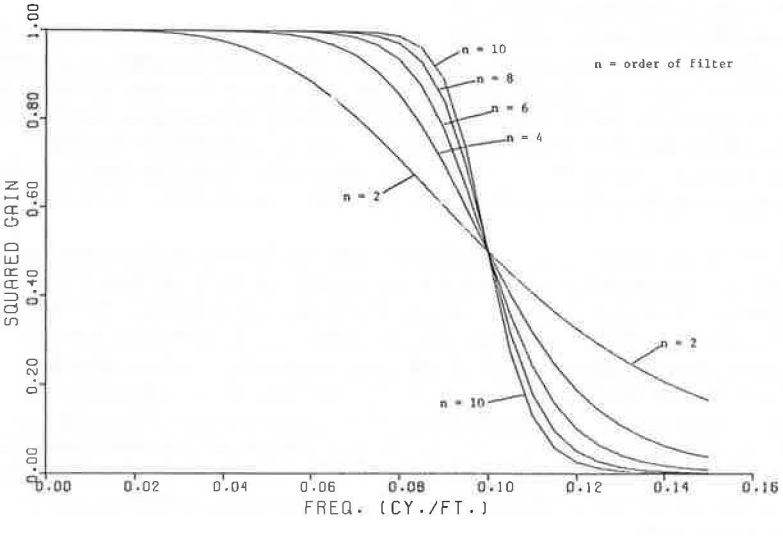

4. Characteristics of the filter can be changed tremendously by varying the order.

Although several other methods, including the digital resonator, certain nonrecursive filters, and moving Fourier transforms, were considered, extensive comparisons among flat-topped recursive filters were not made. In view of characteristics 1 and 4 above and the test results, it is doubtful whether such an investigation would uncover a filter with significant practical advantages over the tangent filter.

ARTIFICIAL TEST CASES

In the following test cases, we will refer only to the tangent form of the squared-magnitude low-pass filter as applied doubly to remove phase shift.

Figures 3, 4, and 5 show the amplitude-smoothing effect for case 1. The artificial test case, zeroes followed by ½ cycle of a sine wave followed by zeroes, is almost unrealistically conducive to filter distortion because of the sharply discontinuous derivatives and the abrupt amplitude changes from 0 to 1 to 0 in successive ½ cycles. This artificial profile, however, resembles a smooth road with an isolated bump and is more realistic than, say, a step function. The difficulties presented and the realism were the reasons for the choice of this test case. Units are intentionally omitted in the figures to emphasize the fact that artificial data are being used. The wavelengths of the signals are given in feet (meters) for convenience and illustration.

The cutoff of the sixth-order filter is at 10 ft (3 m) (Figure 1); therefore the 11.33, 14, and 20-ft (3.45, 4, and 6-m) signals are all in the passband. Thus, the difference between the filtered and unfiltered profiles should be interpreted as distortion introduced by the filter.

The fact that the distortion decreases as the signal's wavelength moves away from the edge of the passband illustrates why extremely narrow-band filters are not adequate: There is no area within the passband sufficiently far from the edges so that excessive distortion is not encountered.

The sharpness of the cutoff is actually less than the gain versus frequency function would indicate when the amplitude variation is great, as given in Table 1.

One might ask whether the results would differ greatly if the sampling rate were decreased or the cutoff frequency were changed; the two questions are really the same: Does changing the number of points per cycle at the cutoff frequency change the results significantly? The test case discussed above was run on 14 and 20-ft (4 and 6-m) wavelength signals with a step size of 2 ft (0.6 m).

The rms values centered at the peak after filtering for the 2-in. (50.8-mm) and 2-ft (0.6-m) cases are, respectively, 0.4492 and 0.4429 for the 14-ft (4-m) signal and 0.4861 and 0.4825 for the 20-ft (6-m) signal. Each rms value is taken over 1 cycle at the wavelength of the signal. The corresponding rms value of a perfectly distortion-free filtered profile would be 0.5 (the value for the unfiltered profile). Thus, a decrease in the sampling rate by a factor of 12 increases the distortion only in the third decimal place. The differences are considered trivial since they are less than the expected measurement errors.

Figures 6, 7, and 8 reveal somewhat improved performance in the less severe test case 2, zeroes followed by 4 cycles of a sine wave with amplitude varying from ½ cycle to ½ cycle. Tables 2, 3, and 4 give the results for test case 2 for the fourth-, sixth-, and tenth-order filters. There is surprisingly little variation from order to order. It can be seen from examining the gain at the frequency of sine wave and the various error measures that, as the order increases, the errors do not decrease as quickly as the gain approaches unity. This is because the amplitude smoothing is exacerbated as the cutoff sharpness increases; i.e., there is a trade-off between distortion due to the nonrectangular gain function and distortion due to amplitude smoothing. The sixth-order filter is recommended as a reasonable compromise considering both distortion and computational efficiency.

It is felt that the rms and the maxima of the errors in the local rms values are adequately small in these test cases chosen to be conducive to filter distortion and to justify use of the sixth-order filter for computing measures of local roughness versus frequency. The test cases with real data in the following section provide further and more convincing evidence.

TEST CASES USING ROAD PROFILES

Although the artificial test cases are useful, real cases such as those discussed below are the ultimate tests. The following points are made in this section:

Figure 3. Filtered and unfiltered profiles for case 1, 11.33-ft (3.45-m) wavelength signal, sixth-order filter.

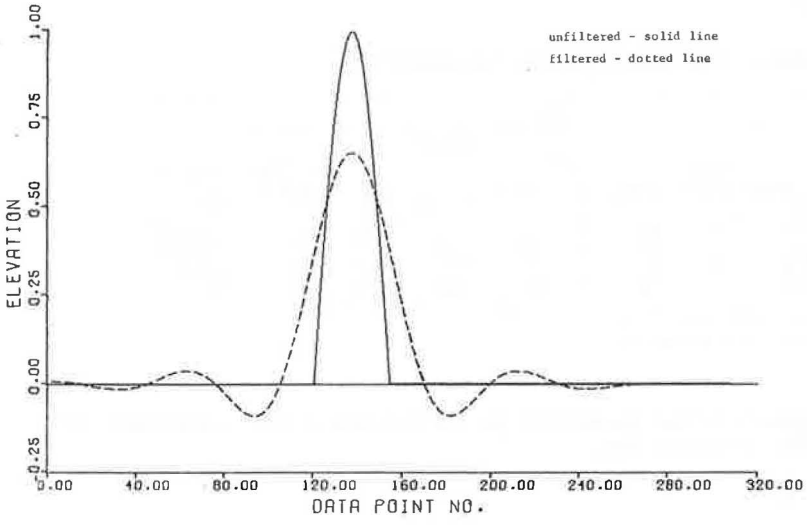

Figure 4. Filtered and unfiltered profiles for case 1, 14-ft (4-m) wavelength signal, sixth-order filter.

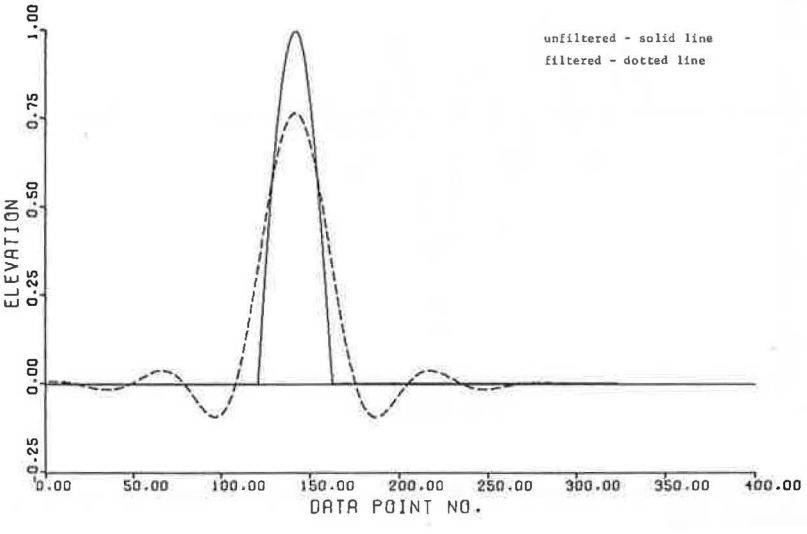

Figure 5. Filtered and unfiltered profiles for case 1, 20-ft (6-m) wavelength signal, sixth-order filter.

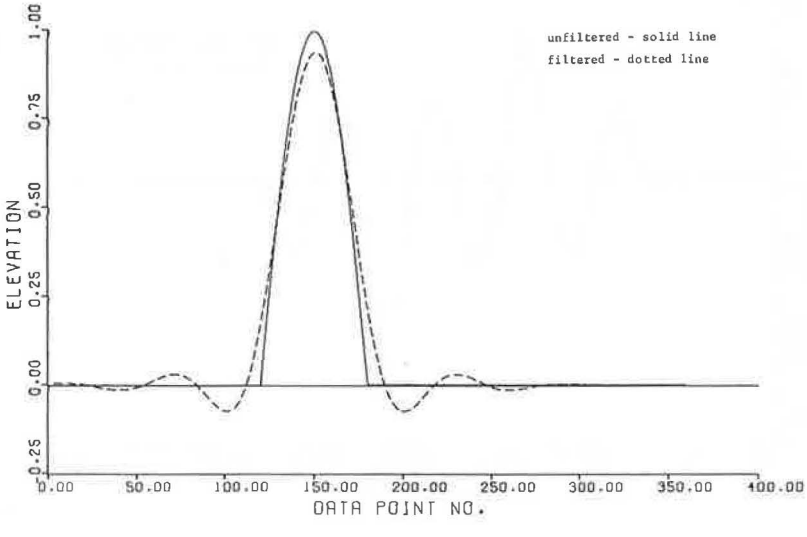

Table 1. Results for test case 1, sixth-order filter.

Frequency (cycle/ft)	Wavelength (ft)	Points/ Cycle	Amplitude: Unfiltered: At Peak	Amplitude: Unfiltered: rms at Peak[a]	Amplitude: Filtered: At Peak	Amplitude: Filtered: rms at Peak	Amplitude: Filtered: At ½ Cycle Past Last Peak	Gain at Frequency of Sine Wave
0.500	2	12	1	0.5	0.125	0.122	0.116	0.0313×10^{-7}
0.250	4	24	1	0.5	0.252	0.231	0.187	0.0158×10^{-3}
0.167	6	36	1	0.5	0.374	0.310	0.163	0.0021
0.125	8	48	1	0.5	0.487	0.363	0.117	0.0639
0.100	10	60	1	0.5	0.591	0.400	0.027	0.5000

Note: 1 cycle/ft = 3.2 cycles/m, 1 ft = 0.3 m.

[a]Taken over 1 cycle at the wavelength of the signal.

Figure 6. Filtered and unfiltered profiles for case 2, 11.33-ft (3.45-m) wavelength signal, sixth-order filter.

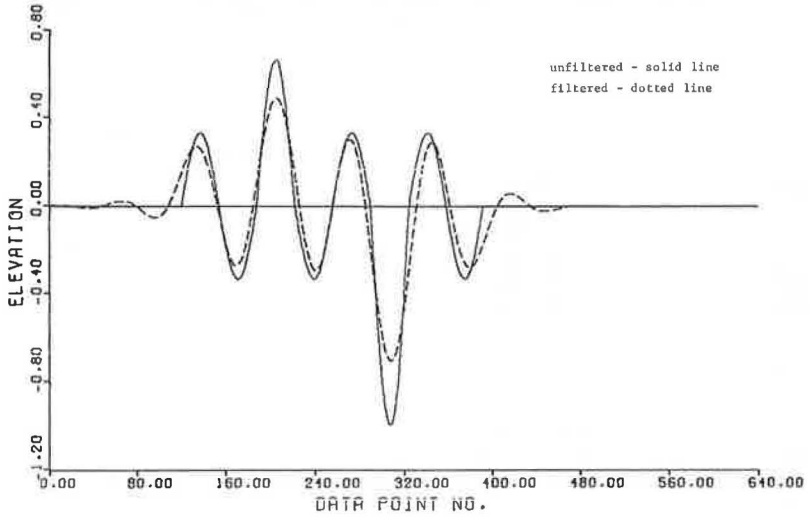

Figure 7. Filtered and unfiltered profiles for case 2, 14-ft (4-m) wavelength signal, sixth-order filter.

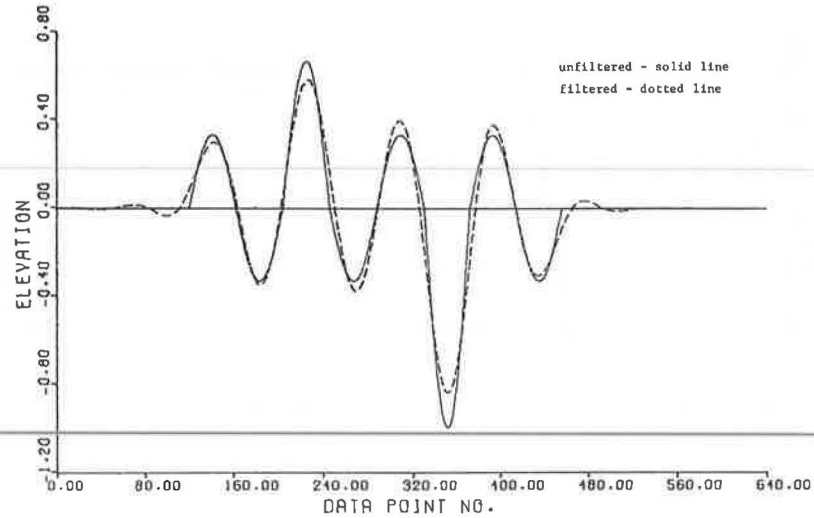

Figure 8. Filtered and unfiltered profiles for case 2, 20-ft (6-m) wavelength signal, sixth-order filter.

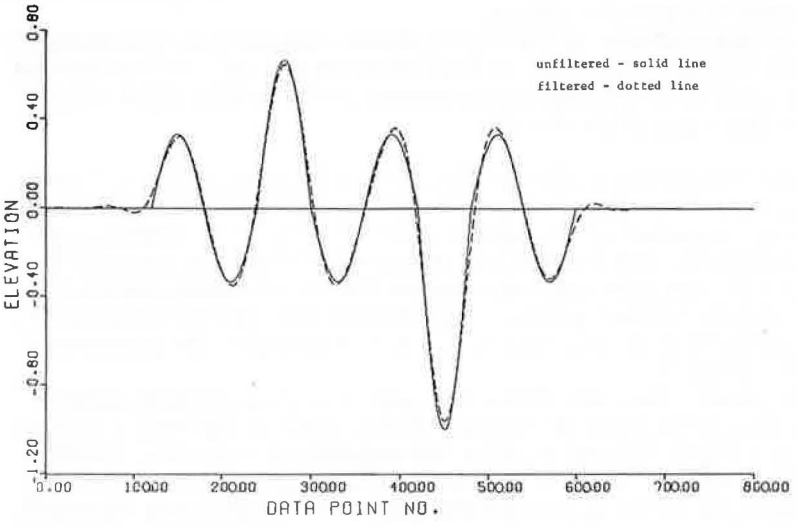

Table 2. Results for test case 2, fourth-order filter.

Item	Wavelength (ft)	Points/Cycle	Filtered Amplitude of ½ Cycles at Peaks 1	2	3	4	5	6	7	8	Error rms[a,b]	Error Maximum[b]	Filtered Amplitude at ½ Cycle Past Last Peak	Gain at Frequency of Sine Wave
Frequency, cycle/ft														
0.088	11.33	68	0.236	0.244	0.464	0.257	0.259	0.681	0.250	0.240	0.078	0.132	0.015	0.732
0.079	12.67	76	0.271	0.298	0.529	0.320	0.329	0.766	0.314	0.278	0.047	0.088	0.029	0.869
0.071	14.00	84	0.289	0.329	0.568	0.346	0.363	0.823	0.352	0.294	0.029	0.059	0.029	0.937
0.060	16.67	100	0.305	0.351	0.611	0.349	0.372	0.896	0.374	0.305	0.014	0.029	0.021	0.984
0.050	20.00	120	0.319	0.345	0.643	0.341	0.355	0.953	0.357	0.318	0.007	0.014	0.011	0.996
Amplitude of input time series			0.333	0.333	0.667	0.333	0.333	1.0	0.333	0.333				

Note:. 1 cycle/ft = 3.2 cycles/m. 1 ft = 0.3 m.
[a]Points from ½ cycle before to ½ cycle after sine waves were used in rms error calculation. [b]Moving values taken over 1 cycle at wavelength of signal.

Table 3. Results for test case 2, sixth-order filter.

Item	Wavelength (ft)	Points/Cycle	Filtered Amplitude of ½ Cycles at Peaks 1	2	3	4	5	6	7	8	Error rms[a,b]	Error Maximum[b]	Filtered Amplitude at ½ Cycle Past Last Peak	Gain at Frequency of Sine Wave
Frequency, cycle/ft														
0.088	11.33	68	0.257	0.268	0.492	0.295	0.294	0.705	0.274	0.264	0.063	0.114	0.036	0.818
0.079	12.67	76	0.288	0.321	0.557	0.363	0.372	0.791	0.343	0.301	0.034	0.071	0.045	0.945
0.071	14.00	84	0.299	0.348	0.584	0.375	0.396	0.840	0.378	0.308	0.022	0.046	0.034	0.983
0.060	16.67	100	0.305	0.365	0.617	0.352	0.384	0.904	0.392	0.302	0.012	0.025	0.021	0.998
0.050	20.00	120	0.321	0.347	0.648	0.340	0.354	0.960	0.359	0.318	0.006	0.013	0.011	1.000
Amplitude of input time series			0.333	0.333	0.667	0.333	0.333	1.000	0.333	0.333				

Note: 1 cycle/ft = 3.2 cycles/m. 1 ft = 0.3 m.
[a]Points ½ cycle before to ½ cycle after sine waves were used in rms error calculation. [b]Moving values taken over 1 cycle at wavelength of signal.

Table 4. Results for test case 2, tenth-order filter.

Item	Wavelength (ft)	Points/Cycle	Filtered Amplitude of ½ Cycles at Peaks 1	2	3	4	5	6	7	8	Error rms[a,b]	Error Maximum[b]	Filtered Amplitude at ½ Cycle Past Last Peak	Gain at Frequency of Sine Wave
Frequency, cycle/ft														
0.088	11.33	68	0.261	0.293	0.518	0.327	0.323	0.721	0.291	0.280	0.054	0.104	0.046	0.925
0.079	12.67	76	0.295	0.330	0.574	0.396	0.403	0.802	0.353	0.309	0.030	0.066	0.053	0.991
0.071	14.00	84	0.302	0.350	0.581	0.388	0.410	0.837	0.384	0.311	0.023	0.047	0.034	0.999
0.060	16.67	100	0.296	0.370	0.608	0.342	0.381	0.893	0.400	0.287	0.014	0.028	0.018	1.000
0.050	20.00	120	0.315	0.336	0.640	0.330	0.347	0.949	0.350	0.312	0.009	0.017	0.014	1.000
Amplitude of input time series			0.333	0.333	0.667	0.333	0.333	1.000	0.333	0.333				

Note: 1 cycle/ft = 3.2 cycles/m. 1 ft = 0.3 m.
[a]Points ½ cycle before to ½ cycle after sine waves were used in rms error calculation. [b]Moving values taken over 1 cycle at wavelength of signal.

1. Plots of filtered and unfiltered profiles demonstrate directly the capability of the methods to isolate a specified type of roughness.
2. Pilot-study results demonstrate the use of roughness measures computed from filtered profiles in comparing new hot-mixed asphalt concrete and new surface-treated roads in Texas. This is important because the measures can be used to infer important differences between two types of pavements.

An asphalt surface-treated section on the Old San Antonio Road near Bryan, Texas, was chosen to illustrate the sixth-order, low-pass filter's performance with real data. The two-lane road is very rough; the serviceability index (9, 10) is 1.7. Swelling clay distress is known to be present. The filtered and unfiltered profiles are shown in Figures 9 and 10. In Figure 10, the difference between the low-pass filtered outputs was used to simulate the band-pass filtered profile. The desired information seems to be portrayed extremely well in the filtered profiles. Note, for example, the pronounced long waves in Figure 10, frame 2.

Although the high-frequency waves are shown in Figure 9 to be accurately isolated by the filter, there are occasional curious-looking results, such as the large v in Figure 9, frame 1, at about a 335-ft (102-m) position that appears as a shorter, smaller amplitude v in the filtered profile. The v in the raw profile is apparently interpreted by the filter as a long wave not in the passband with short waves (composing the small v) in the band. Generally, because of the presence of many waves superimposed, visual filtering to see what the digital filter should and should not respond to is difficult. The step size for the test cases using road profiles is 0.169 ft (0.05 m) [about 2 in. (50.8 mm)] for each wheel path.

Finally, as an example of an application of filtering, we consider selected results from a pilot study in which new (less than 1-year-old) hot-mixed asphalt concrete pavements were compared to the less expensive surface-treated pavements. All sections were either new or rebuilt except for one of the hot-mixed sections, which had an overlay on an existing structure. The two samples contained 10 hot-mixed and 11 surface-treated sections; each 1,200-ft (366-m) section was from a different project. The projects are distributed over the state of Texas.

The mean serviceability indexes for the surface-treated and hot-mixed samples are 3.5 and 3.9 respectively. The ranges for the two samples are 2.7 to 4.1 and 3.5 to 4.5 respectively. Further information on the sections is given elsewhere (3). Because of the limited nature of the study, the results are presented as illustration, not as conclusive findings.

For (the filtered output for) a given passband, calculations are done for each of the two samples as follows:

1. Recursively compute the local rms amplitude for the right, left, and pointwise difference profiles at each step throughout the section. The rms values are taken over 1 cycle at the longest wavelength in the passband.
2. Compute the 50th, 75th, 90th, 95th, and 99th percentile points of each of the three sets of local roughness measures. The q th percentile point is the value greater than or equal to exactly q percent of the set of rms amplitudes in question (compare with 1). The 50th percentile amplitude, being greater than exactly half of the moving rms values, is the median of the local amplitudes. Thus, the 50th percentile value is the average roughness in the road section. The 95th percentile is greater than exactly 95 percent of the local rms amplitudes. Thus, the local roughness is worse than the 95th percentile value only 5 percent of the time, and the 95th percentile value indicates how bad the most severe roughness in the section is.
3. Average the corresponding right and left percentile amplitudes yielding a set of measures of longitudinal roughness. The pointwise difference percentile amplitudes are measures of transverse roughness.
4. Compute the sample mean and the standard deviation of the mean for each roughness measure, e.g., the 75th percentile amplitude for longitudinal roughness.

Calculations 1, 2, and 3 were done for each section separately.

Figure 9. Filtered and unfiltered profiles for Old San Antonio Road, 0 to 10-ft (0 to 0.3-m) wavelength signal, sixth-order signal.

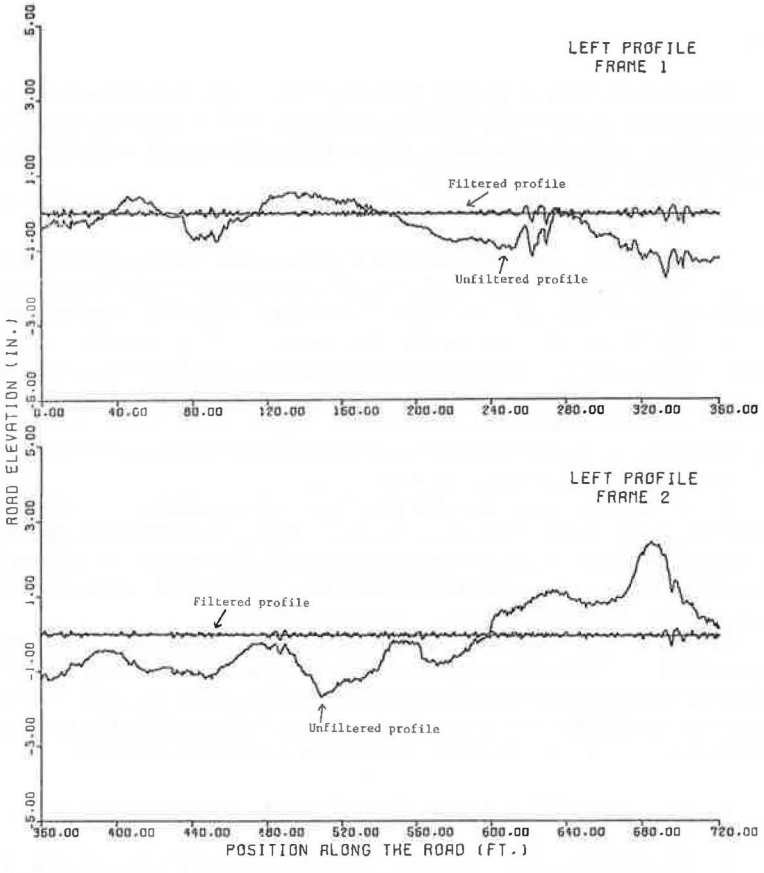

Figure 10. Filtered and unfiltered profiles for Old San Antonio Road, 60 to 100-ft (18 to 30.5-m) wavelength signal, sixth-order signal.

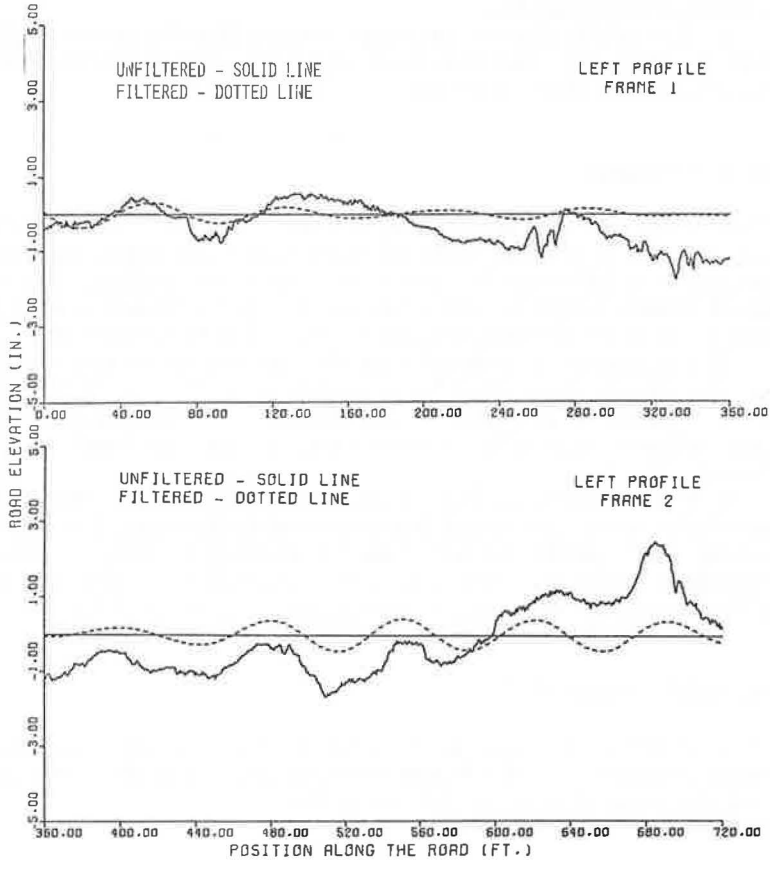

The means and ±1 sigma bars for the means are shown in Figures 11 and 12. Comparisons are made graphically, rather than through the more conventional t- and F-statistics, to facilitate clear illustration of several relationships that can be studied through this type of analysis.

From Figure 11, we note the following facts about the 0 to 1-ft (0 to 0.3-m) passband:

1. Roughness amplitudes are significantly larger for the surface-treated roads.
2. Confidence bars indicate that the sample of surface-treated roads (S) is much more diverse than the sample of hot-mixed asphalt concrete roads (H).
3. Both samples are more diverse at the high percentile points than at the 50th percentile points. This is probably due in part to larger sampling errors in the high percentile amplitudes. Further study is needed to determine the sampling distributions of the various roughness measures. Thus, the variation in the road sections with respect to the presence of a few severe places is greater than the variation with respect to the average roughness in a section.
4. Difference between the two types of pavements is much greater at the high percentile points than at the low points. Thus, the surface-treated roads have a much greater tendency than the hot-mixed asphalt concrete roads to have a few very severe bumps. The surface-treated roads are also worse with respect to overall section roughness, but the difference is not so great.
5. For either sample, the transverse amplitudes are larger than the longitudinal amplitudes. This was expected; for very short wavelengths, a transverse rms amplitude is analogous to the standard deviation of the difference between two independent random variables; however, the right or left amplitudes are analogous to the standard deviation of one or the other of the two random variables.

From Figure 12, we note the following facts about the 27 to 81-ft (8 to 25-m) passband:

1. Confidence bars overlap, indicating that the two types of pavement (S and H) do not differ significantly.
2. Longitudinal amplitudes are greater than the cross amplitudes for the longer waves. This was expected, since the right and left profile fluctuations are positively correlated for the long waves.

CONCLUSIONS

The recursive filter designed by the tangent form of the squared-magnitude approximating function is recommended for use in analyzing road profiles. Although there is surprisingly small order-to-order variation in the artificial test cases chosen to study local transient effects, the sixth-order filter is recommended because it has acceptably sharp cutoff characteristics and is computationally efficient.

The distortion introduced near the edges of the filter passband when the input road profile varies significantly in amplitude from ½ cycle to ½ cycle must be kept in mind. It is probably futile to expect to estimate, with high accuracy, the local amplitudes of the surface irregularities within a very narrow passband, e.g., 30 to 33 ft (9 to 10 m) in wavelength.

It is felt, however, that the artificial test cases, which were chosen to be highly conducive to filter-induced distortion and to illustrate the types of transient effects to be expected, justify the use of digital filtering to compute measures of local amplitude versus wavelength. Probably more important is the fact that the chosen sixth-order filter gave realistic results when applied to road profiles.

ACKNOWLEDGMENT

This study was carried out at the Center for Highway Research in Austin. I wish to thank the sponsors, the Texas State Department of Highways and Public Transportation and the Federal Highway Administration.

Figure 11. Root-mean-square amplitude versus percentile level longitudinal roughness for 0 to 1-ft (0 to 0.3-m) passband.

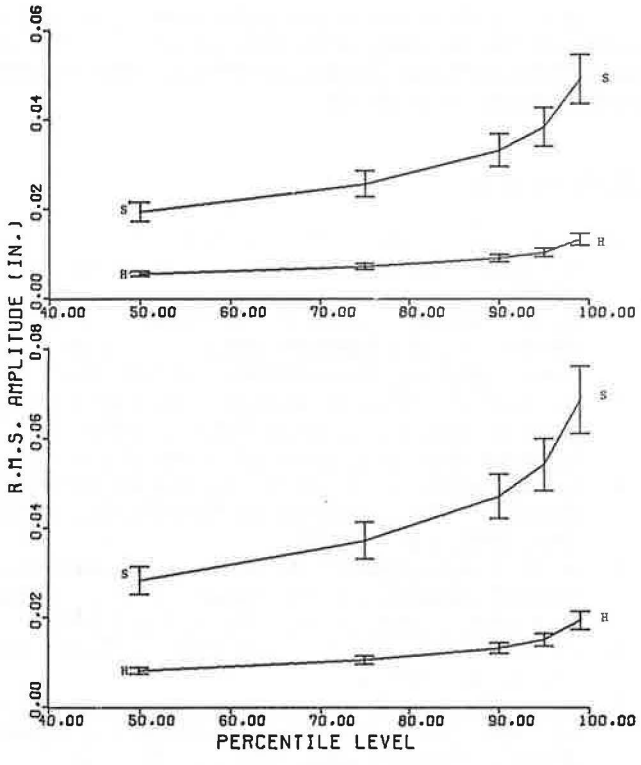

Figure 12. Root-mean-square amplitude versus percentile level longitudinal roughness for 27 to 81-ft (8 to 25-m) passband.

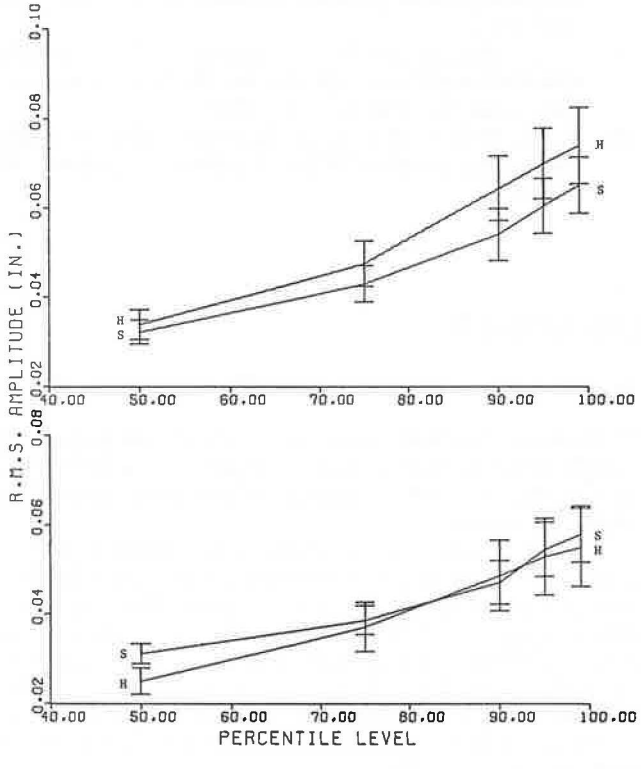

The contents of this paper reflect the views of the author, who is responsible for the facts and the accuracy of the data presented. The contents do not necessarily reflect the official views or policies of FHWA. This report does not constitute a standard, specification, or regulation.

REFERENCES

1. A. D. Brickman, J. C. Wambold, and J. R. Zimmerman. An Amplitude-Frequency Description of Road Roughness. HRB Special Rept. 116, 1971, pp. 53-67.
2. L. F. Holbrook and J. R. Darlington. Analytical Problems Encountered in the Correlation of Subjective Response and Pavement Power Spectral Density Functions. Highway Research Record 471, 1973, pp. 83-90.
3. M. Holsen and W. R. Hudson. Stochastic Design Parameters and Lack-of-Fit of Performance Model in the Texas Flexible Pavement Design System. Center for Highway Research, Univ. of Texas at Austin, Research Rept. 123-23, April 1974.
4. C. M. Rader and B. Gold. Digital Filter Design Techniques in the Frequency Domain. Proc., Institute of Electrical and Electronics Engineers, Vol. 55, No. 2, Feb. 1967, pp. 149-171.
5. F. L. Roberts and W. R. Hudson. Pavement Serviceability Equations Using the Surface Dynamics Profilometer. Center for Highway Research, Univ. of Texas at Austin, Research Rept. 73-3, April 1970.
6. J. L. Shanks. Recursion Filters for Digital Processing. Geophysics, Vol. 32, No. 1, pp. 33-51.
7. R. S. Walker, F. L. Roberts, and W. R. Hudson. A Profile Measuring, Recording, and Processing System. Center for Highway Research, Univ. of Texas at Austin, Research Rept. 73-2, April 1970.
8. R. S. Walker and W. R. Hudson. Practical Uses of Spectral Analysis With the Surface Dynamics Road Profilometer. Highway Research Record 362, 1971, pp. 104-119.
9. R. S. Walker and W. R. Hudson. The Use of Spectral Estimates for Pavement Characterization. Center for Highway Research, Univ. of Texas at Austin, Research Rept. 156-2, Aug. 1973.
10. R. S. Walker and W. R. Hudson. Use of Profile Wave Amplitude Estimates for Pavement Serviceability Measures. Highway Research Record 471, 1973, pp. 110-117.

DISCUSSION

B. E. Quinn, Mechanical Engineering School, Purdue University

Williamson has demonstrated a way of comparing pavement profiles by filtering various wavelengths from the profile in question and then by comparing the filtered results. In some respects this is similar to pavement spectrum analysis with which I have had some experience.

If an analysis is to be made of the extent to which various wavelengths are found in a pavement profile, the question about what filtering technique to use inevitably arises. The problems of filtering highway profiles provide more of a challenge than certain other types of data because an enormous range of wavelengths exists in a pavement profile, where wavelengths from a few feet (meters) to several hundred feet (meters) may exist together. The problem is further complicated because the long wavelengths usually have a much greater amplitude than the shorter wavelengths. I have observed approximately five orders of magnitude difference in the wavelengths that exist in certain pavement profiles.

The existence of this large variation in amplitudes complicates the filtering process which, as Williamson shows, is never perfect. The mathematical filters never exclude all of the side-band frequencies as his filter characteristics so clearly show. One complication arises because a very small percentage of a side-band frequency having an amplitude several orders of magnitude larger than the frequency of interest may introduce into the filtered results an effect having the same order of magnitude as the band of wavelengths under consideration.

I prefer making a pavement roughness spectral analysis, but in either case this filtering problem is encountered because spectral analysis can usually not be made on pavement elevation profiles when some type of preliminary data processing procedure has not been applied to the profile.

I have experimented with different filters to remove the long pavement wavelengths. A variety of results could be obtained depending on the filtering technique used. Moreover, each filtering technique produced its own distortion in the filtered results thus causing additional problems. The question can therefore be asked about what type of filtering process is appropriate when pavement profiles are studied. This may depend on the use that is to be made of the filtered results; in this case the dynamic tire forces in passenger vehicles were to be predicted. A variety of pavement roughness spectra could be obtained as inputs to the mathematical model depending on the filtering procedure used for processing the elevation measurements. In this case, the question was resolved by measuring the dynamic tire forces experimentally and by computing the spectral density of the dynamic tire forces from the force-time histories. These records did not contain the enormous variation in frequency nor the corresponding large variation in amplitude that existed in the pavement profiles. As a result, the filtering procedure was not as critical for these data as it was for the profile. The power spectrum of the dynamic tire forces was then computed by using a mathematical model in which the pavement roughness spectrum was included as the input and in which the vehicle characteristics were represented.

The pavement roughness spectrum when used with the vehicle characteristics did not give a dynamic tire force spectrum that agreed particularly well with the spectral analysis of the dynamic tire force data obtained experimentally. This was particularly true in the high-frequency region because the elevation measurements used to define the pavement profile were not accurate enough when used with this type of analysis to predict the vehicle behavior. This was true because the vehicle was very sensitive to pavement excitation at the wheel-hop frequency. No filtering could improve the original accuracy of the elevation measurements, and only experimental data revealed the limits to the usefulness of the frequency analysis of the pavement profiles.

It is possible to make frequency analyses of road profiles by using many different types of filters. A basic problem that must be resolved however is that of determining which wavelengths are significant in the profile and to what degree of accuracy they must be determined.

In my opinion, the evaluation of a pavement profile must be related to the vehicle that will be using the pavement and to the velocity at which the vehicle will be operated. Objective criteria can then be obtained that make it possible to determine whether a pavement is either good or bad.

DISCUSSION

Arthur D. Brickman, Department of Mechanical Engineering,
Pennsylvania State University

Williamson is to be commended for describing a detailed mathematical investigation most lucidly and for showing how data analysis can reduce an apparently endless random profile measurement to a few simple graphs. In developing and testing the analysis scheme, however, he has made some decisions that bear further justification:

1. A reverse filtering procedure is applied to the input profile to eliminate phase-shift effects from the filtered profile. Since we are concerned with relatively narrow passband filtering in which the passed signal components all have about the same lag and since we subsequently look only at the amplitude characteristics of the filtered profile, why is this special procedure necessary? If the input profiles are measured by the GM profilometer, they already contain some inherent phase-shift effects at the longer wavelength components because of the on-board filter typically used in profile taping.
2. Although the ½ sine pulses used as test inputs for the digital filter do emphasize its limits of accuracy, these signals are difficult to associate with typical roughness singularities that appear on actual profile records. It would be instructive to see what the filter response would be to more realistic inputs such as a modified single step (slab edge), ramp (bridge approach), and versine (single smooth bump). Comparative filter response results for such inputs have been observed in other investigations including those of the GM profilometer (11).
3. The end result of processing a roughness profile by using Williamson's method is a graph that shows the cumulative distribution of roughness amplitudes to be expected in a given range of roughness wavelengths for a given road. Thus, a complete description of the roughness by this method involves a family of curves covering all the wavelength bands of interest. What advantages does this system for describing road roughness have over existing methods (12) based on analog filtering and amplitude counting?

Part of the analysis system described by Williamson involves computation of a transverse roughness characteristic based on the difference between the right and left wheel path profiles. This presumably relates to a possible roll type of excitation of the traversing vehicle due to road roughness. An interesting extension of this would be to find another type of difference based on the instantaneous difference between the profile as experienced by the front and rear wheels. It would appear that the digital techniques used in the investigation could be readily adapted to obtaining and analyzing this wheelbase roughness. If so, the complete characterization of a road profile could include longitudinal, transverse, and fore-and-aft values corresponding to the heave, roll, and pitch modes of possible vehicle vibration. Such a roughness description would be extremely useful for determining road user satisfaction as mentioned by Williamson.

REFERENCES

11. E. B. Spangler and W. J. Kelly. GMR Road Profilometer: A Method for Measuring Road Profile. General Motors Corp., Research Publ. GMR-452, Dec. 22, 1964, pp. 8-14.
12. J. C. Wambold and J. R. Zimmerman. Hybrid Programs for Calculating the Joint Probability of Amplitude and Frequency of a Random Signal. Trans., Analog/Hybrid Computer Education Society, West Long Branch, N.J., Vol. 3, No. 7, July 1971, pp. 133-144.

AUTHOR'S CLOSURE

I appreciate the perceptive comments made by both reviewers. Quinn has added some valuable discussion from his experience about practical considerations in the signal processing of road profiles and related time series. His discussion of the problems that can be caused by amplitudes that change sharply with frequency, for example, is an excellent supplement to the brief comments made on this subject in the paper. Because of this and other pitfalls discussed, I strongly recommend side-by-side comparison of measured and filtered profiles for a representative set of cases to verify that a given

filtering scheme does not introduce excessive distortion.

Brickman has raised some valid questions for discussion. My responses correspond to his specific points as follows:

1. If only band-pass filters with narrow passbands were to be used and if only amplitude characteristics were of interest, then the phase shift would probably not be important. It is true also that the analog filters on the GM profilometer induce a phase shift in the longer waves. For the vehicle speed of 20 mph (32 km/h) and the two filter selections most commonly used in our work, the phase shifts begin at about 30 and 60 ft (9 and 18 m) in wavelength. There are some applications, however, for which the location of specific short waves might be important, such as the study of roughness on the approaches and at the ends of bridges and the study of roughness associated with joints in concrete pavements. Furthermore, the convenience of examining measured and filtered profiles plotted in the same figure requires that there not be a phase-shift difference between the two profiles. This type of visual analysis, which was used in the paper to demonstrate filter characteristics, can also be valuable in studies of pavement properties such as those mentioned above. It may appear that the requirement of double filtering is an excessive computational burden. A double filter, however, has much sharper cutoff characteristics than the single filter on which it is based; the gain at a given frequency of the double filter is the square of the gain of the single filter. Thus, to achieve a certain degree of frequency resolution, the order required for a double filter is lower than the order that would be required if the filter were to be applied only once. This is significant because the number of terms required increases linearly with the order, but the incremental frequency resolution decreases with order. In addition, even though a phase shift is present for longer waves, the accuracy of the analysis is not improved by the introduction of phase shifts for all waves. Although in many applications the phase-shift effect may not be serious, it is a source of distortion, and since it is easily eliminated, there seems to be no reason to include it.

2. Artificial profiles were used because sufficiently realistic and difficult test cases with a known answer could be associated and provide meaningful comparisons. It is felt that the ½ sine waves, which resemble an isolated bump on an otherwise smooth road, and the cases with 4 sine waves with varying amplitudes served this purpose. Additionally, these test cases involving only a single frequency were convenient for studying the relationship between filter distortion and nearness of frequency to the edge of the passband.

Real road profiles provide more realistic tests than any artificial profile could provide. This is the reason for the inclusion of plots showing both the measured and the filtered profiles and the discussion of the adequacy of the filter on the basis of the plots. Brickman has suggested some interesting possibilities for further testing with artifical data, however. The smooth bump in particular is similar to, but more realistic than, the ½ sine wave. Even if it were composed only of a part of a single sine wave, however, the smooth bump would involve other frequencies. Consider

$$f(x) = 1 + \sin(x) \quad \text{if } -90 \text{ deg} < x < 270 \text{ deg}$$

$$= 0 \quad \text{if otherwise} \tag{3}$$

The unit step, which is added to achieve continuity, introduces frequency components other than that of the sine wave. Thus, if only for the purpose of studying the relationship between distortion and nearness of the frequency to the edge of the passband, the test cases that were used have some value.

3. Amplitude frequency distribution (AFD) (1) is apparently closely related to another method (12). I am in basic agreement with the AFD approach, since it provides an effective means for evaluating the amplitude variation as well as the average or overall roughness in a road section. The statistical approach I used is essentially the same as that used in the AFD method except that the distribution of a local roughness

measure, the rms of the filtered elevations over 1 cycle at the longest wavelength in the passband, is investigated instead of the distribution of the peaks in the filtered profile. The local roughness measures were used because the local rms values have smaller errors than the filtered values at the peaks (Tables 1 and 2). In Table 2, for example, the maximum error in the moving rms values is considerably smaller in each case than the error in the filtered value at the largest peak. Although these results were obtained with artificial data, the same effects should be expected in real cases because of the nature of the amplitude-smoothing effect. Although I prefer the use of local roughness measures for the reasons state above, the AFD approach is a natural and valid means of characterizing the roughness.

Brickman is right that the wheelbase roughness is important because of the special type of motion it induces in passing vehicles. This could perhaps be handled by including in the analysis a filter passband whose wavelengths spanned the range of values of twice the wheelbases of standard automobiles.

CORRELATION OF OBJECTIVE AND SUBJECTIVE BUS-RIDE RATINGS

William H. Park and James C. Wambold, Pennsylvania Transportation Institute, Pennsylvania State University

This paper describes research concerning the establishment of a correlation between objective and subjective comfort ratings of vehicles traversing rough roads. The absorbed power comfort criterion was used in an amplitude-frequency-distribution format for the objective measure. The objective ratings were then correlated with passenger subjective responses obtained on a city bus traversing 17 distinct road segments. The correlation of absorbed power as an objective ride measure to the subjective evaluation for the bus data was successful. For some individual bus rides, the correlations were poor, but, when a sufficient number of rides were used to give a reasonable sample base, an excellent correlation was obtained and can be expressed mathematically as a logarithmic function. Finally, preliminary correlation of absorbed power with International Standardization Organization standards further enhanced the bus ride and absorbed power correlation numbers since the absorbed powers obtained were of the same order of magnitude for both correlations. Although it would then appear that one could just use International Standardization Organization standards, there is no way to add the effect of multidegrees of freedom. On the other hand, the absorbed power provides a method of adding the effects due to the three major directions plus the pitch and the roll.

•THE object of this research was to use vehicle acceleration versus time data to evaluate ride quality for the vehicle guideway system. The amplitude frequency distribution (AFD) techniques (1, 2, 3), as applied to the absorbed power (AP) (4, 5, 6) method of comfort evaluation previously used in automobile-road roughness studies by the investigators (7, 8, 9), were extended to include 3 degrees of freedom. This extended method was used to evaluate the subjective ride and acceleration data taken by researchers on a city bus. The subjective and objective ride ratings were then correlated (10).

BASIC STATISTICAL MEASURES

Measured records must be recognized as random signals of finite duration and, as such, they can be viewed and described in terms of three basic domains: time, amplitude, and frequency. At first glance, it would appear that the power spectral density (PSD) contains a complete description of amplitude variations, thus making any amplitude-distribution calculations superfluous. However, the ordinate of a PSD curve indicates only the average signal amplitude at a particular frequency. A large PSD value can conceivably be produced by either a few cycles of large amplitude or a large number with small amplitudes; the distinction cannot be made from the PSD curve alone. On the other hand, it is not possible to extract any information about frequency distribution from amplitude density curves. It is evident from these considerations that the PSD and amplitude density curves each contain unique information, and a simple method of combining the two representations is desirable.

An effective method for combining the information contained in both the PSD and the amplitude representations is to reduce the random time-history signal to a simple

tabular array that displays both the height and the length features of the random data, the AFD (1, 2, 3). Here the coordinates (linear or logarithmic), amplitude [in feet (meters) or g] versus frequency [in hertz, revolutions per minute, or cycles per foot (per meter)], are divided into a number of finite bands. Numbers are computed and entered at each windowlike intersection of the bands. The numbers express the total number of signal peaks with the amplitude and frequency of that box in the array. The complete array of numbers thus identifies the random signal as a combined amplitude and frequency distribution. Thus, the AFD not only gives the frequency distribution but also shows the amplitude makeup and distribution of each frequency band.

CORRELATION OF OBJECTIVE WITH SUBJECTIVE RIDE RATINGS

Objective Ride Criterion

Objective ride measures used in this study are based on the concept of AP. This criterion was developed by researchers at the Army Tank Automotive Command (4, 5, 6) and is based on an energy flow rate that depends on the anatomical properties of the human body. The human body properties were determined experimentally, and AP was related to passenger subjective responses.

The information needed for the determination of AP is the acceleration at the interface of the passenger and the vehicle. The experimental data that were used as input had been obtained before initiation of this project and consisted of three-directional accelerations measured on the floor of a bus by using National Aeronautics and Space Administration (NASA) instruments. These accelerations in the vertical, longitudinal, and lateral directions were measured near the front of the bus and simultaneously near the center of the bus and were recorded on magnetic tape. Unfortunately, these accelerations were not measured at the passenger-seat interface but were used because of their availability in this initial project to determine the degree of correlation between the AP criterion and subjective passenger response. Impedance tests were run on the bus seats, and it was determined that their acceleration transfer functions were very close to unity in the frequency range of interest. This permitted the floor data to be used without modification. Other seats might not perform in this manner and may attenuate the signal near the body resonances. Therefore, all future comfort measurements should be made at the passenger-seat interface, or, if this cannot be done, seat transfer characteristics must be determined for each case and included in the analyses if the characteristics dictate it.

AP can be computed from the acceleration data in either the time or the frequency domain for each direction. Since power is a scalar quantity, the total power can be obtained by summing the power in all three directions. For this study, the frequency method was used since the results would reveal those frequency bands that contribute to the greatest discomfort. The format for the calculations is shown by the following equation:

$$\text{average AP} = \sum_{i=0}^{N} K_i A_{i_{rms}}^2 \tag{1}$$

where

AP = absorbed power in watts,
$A_{i_{rms}}^2$ = root-mean-square of the acceleration at a given frequency, and
K_i = parameter used to transform the acceleration squared into AP at a given frequency.

Before the calculation details are given, the AFD concept for formatting the data will be presented.

Amplitude Frequency Distribution Format for Absorbed Power

The AFD method has been found useful in making comfort measurements because it readily identifies both amplitude and frequency bands of the acceleration inputs that are causing the discomfort to the vehicle passenger. Details of this method, which can be used directly on road roughness data, are given elsewhere (7). The acceleration data (either measured or determined from road roughness) for each of the three directions were filtered into eight frequency bands, and peaks were placed in six amplitude bands.

The seat acceleration AFD is the beginning point for comfort evaluation by the AP method. Equation 1 shows that the total AP for a vibration spectrum is the summation of the power at each frequency. The K_i values are for frequencies in hertz, which can be obtained by multiplying the midfrequency by the vehicle speed in feet (meters) per second. Since each block of the seat acceleration AFD has a midamplitude and a midfrequency value, the average AP attributable to each AFD can be calculated from equation 1. The resultant AP matrix is given in Table 1. This value of AP shown in each block, however, would be the power absorbed by a passenger subjected totally to an acceleration of that midfrequency and midamplitude value. Therefore, to account for the fact that the actual acceleration consists of various frequencies and amplitudes, the AP matrix is normalized by dividing each block by the maximum number of counts that would be shown by a sine wave of that midfrequency for that length of time. For example, the last column has a midfrequency of 11.314 Hz. Any amplitude sine wave of that frequency would produce 169.7 counts in that time. These numbers of counts could be termed M_i and are calculated for each frequency. By dividing the AP matrix by the M_i values, a new matrix is obtained that will be called the normalized absorbed power matrix (NAPM). Each block of the NAPM is then $K_i A_i^2/M_i$, which is equal to the AP contribution per count of the seat acceleration AFD. These values are given in the matrix in Table 2. The NAPM shows those areas that contribute the most to AP (or discomfort) and, thus, gives a picture of the amplitudes and frequencies that contribute to a comfortable ride.

For determination of AP for a particular ride segment, NAPM is multiplied block by block with the seat acceleration AFD to give the absorbed power AFD (APAFD) as given in Table 3. The APAFD gives the amount of power attributed to each frequency and amplitude block for the guideway and vehicle being examined. The AP for each frequency band can then be obtained by summing the blocks vertically, or the total AP can be obtained by summing all the blocks. The absorbed power AFDs for all segments for each ride are given elsewhere (10).

Correlation Method for Objective and Subjective Ride Ratings

Subjective ride ratings from the bus study were given by the two passengers seated directly over each instrument package used to record the floor accelerations. The correlation simply consisted of plotting the total AP for all three directions against the ride rating number assigned by the passenger.

TEST DATA PROCESSING

The computational program was developed for a hybrid computer in the College of Engineering of Pennsylvania State University. When a random signal has been stored, in continuous analog form on FM tape, or in discrete digitized form on IBM tape, processing the signal to determine its amplitude frequency distribution demands performance of two distinguishable but serially connected operations. The signal must be filtered in each of a number of narrow bandpass filters, and the amplitude peaks must be discriminated and counted for each filter's output. The technique used is shown in Figure 1.

To get a fairly precise characterization of the amplitude frequency distribution of a

random signal requires quite a few relatively narrow (about an octave or less) frequency bands. This need presses against the limitations of cost and availability of hardware. Processing time is reduced dramatically if a random signal can be fed into a parallel set of filters that yields simultaneously the filtered outputs for all filter bands.

When the output of a bandpass filter is available, the peak discrimination can be done. For a narrow bandpass filter the output is a quasisinusoidal signal with fairly uniform frequency but with varying amplitude. The function of peak discrimination is to detect when a peak has occurred, to determine in which of a spectrum of discrete amplitude levels the signal has peaked, and to record this even by updating an appropriate counter. The outputs of the several filters are digitized, and the peak discrimination and counting are done by purely digital means.

Hybrid Absorbed Power Program Method

The files created by the digitizing program are used by the AFD program. The peaks in the amplitude of the data are then found by comparing each digital sample with the sample preceding it and the one following it, until a maximum in the amplitude is found. For each cycle in the amplitude of the data, the peak value is found and stored in an array. In addition, the time in seconds (since the beginning of the test run) at which the peak occurred is also stored in the array. Insignificant amplitude peaks, down in the noise level, are ignored. Data are then printed out in a listing that gives the amplitude of each peak in the data, the time of the peak occurrence, the unadjusted AP, and the AP contributed by the peak. One such listing is provided for each frequency band of each degree of freedom. The peaks are now discriminated into the amplitude bands for the AFD, and the value of each peak is compared with the upper amplitude levels of the amplitude bands, starting with the lowest. Each amplitude band is tested until the upper level of that band exceeds the value of the peak. The number in the AFD array whose position is determined by that amplitude band and the frequency band being processed is then increased by 1. In this way, the number of peaks having each particular combination of amplitude and frequency can be determined. The unadjusted APAFD is then calculated by multiplying the number of peaks in the AFD for each amplitude-frequency combination by the square of the center amplitude of that amplitude band and then by multiplying this by the proper K factor for that frequency band. APAFD is calculated by dividing each value in the unadjusted APAFD by the maximum number of counts that could have occurred during the test run by a continuous sine wave having a frequency equal to the center frequency of the band containing the value. The AFD, unadjusted APAFD, and APAFD are printed out for each degree of freedom.

Objective Ride Data

Results obtained by processing the bus ride data are discussed in the following. The first part of the output listing gives the amplitude and frequency bands selected. This listing provides band limits, and, depending on the scales chosen (linear or log), the center frequencies and amplitudes are calculated and listed. This listing is not repeated until the next computer run when a different set of bands can be chosen.

The next part of the computer output consists of eight listings, one for each frequency band of each segment of bus data. The first column gives the time in seconds, after the beginning of the segment, at which a peak in the acceleration amplitude occurs. The second column gives the amplitude of this peak, and the third column gives the unadjusted AP which is used as an intermediate step in calculating AP. The fourth column gives the AP contributed by the amplitude peak. This is the actual power absorbed by the passenger because of this acceleration peak. This listing contains only those peaks with an acceleration amplitude of at least 0.02 g, so that insignificant peaks with small AP values are ignored. The listing is provided so that the time and amplitude of those peaks contributing large AP values can be identified. Table 4 gives a typical listing from run 7, segment 3, vertical motion, from front accelerometers.

Table 1. Absorbed power matrix for run 8, vertical motion.

Midacceleration (g)	Midfrequency (Hz)							
	0.088	0.177	0.354	0.707	1.414	2.828	5.657	11.314
0.401	0.00682	0.02746	0.11024	0.46851	2.04678	10.10910	12.14340	3.03440
0.257	0.00281	0.01132	0.04543	0.19309	0.84354	4.16625	5.00465	1.25056
0.165	0.00116	0.00466	0.01872	0.07958	0.34765	1.71703	2.06256	0.51539
0.101	0.00048	0.00192	0.00772	0.03280	0.14328	0.70764	0.85004	0.21241
0.069	0.00020	0.00079	0.00318	0.01352	0.05905	0.29164	0.35033	0.08754
0.044	0.00008	0.00033	0.00131	0.00557	0.02434	0.12019	0.14438	0.03608

Table 2. Normalized absorbed power matrix for run 8, vertical motion.

Midacceleration (g)	Midfrequency (Hz)							
	0.088	0.177	0.354	0.707	1.414	2.828	5.657	11.314
0.401	0.00515	0.01035	0.02079	0.04417	0.09849	0.23827	0.14311	0.01788
0.257	0.00212	0.00427	0.00857	0.01820	0.03976	0.09820	0.05898	0.00737
0.165	0.00087	0.00176	0.00353	0.00750	0.01639	0.04047	0.02431	0.00304
0.101	0.00036	0.00072	0.00146	0.00309	0.00675	0.01668	0.01002	0.00125
0.069	0.00015	0.00030	0.00060	0.00127	0.00278	0.00687	0.00413	0.00052
0.044	0.00006	0.00012	0.00025	0.00053	0.00115	0.00283	0.00170	0.00021

Table 3. Absorbed power amplitude frequency distribution determined from experimental acceleration for run 8, segment 1, vertical motion.

Midacceleration (g)	Midfrequency (Hz)							
	0.088	0.177	0.354	0.707	1.414	2.828	5.657	11.314
0.401	0.000	0.000	0.021	0.044	0.000	0.000	0.000	0.000
0.257	0.000	0.004	0.000	0.000	0.000	0.000	0.000	0.000
0.165	0.000	0.002	0.004	0.000	0.000	0.000	0.000	0.003
0.101	0.000	0.000	0.000	0.003	0.000	0.000	0.000	0.010
0.069	0.000	0.000	0.001	0.000	0.008	0.000	0.004	0.023
0.044	0.000	0.000	0.000	0.001	0.002	0.008	0.017	0.011

Figure 1. Determining joint probability density of random signal.

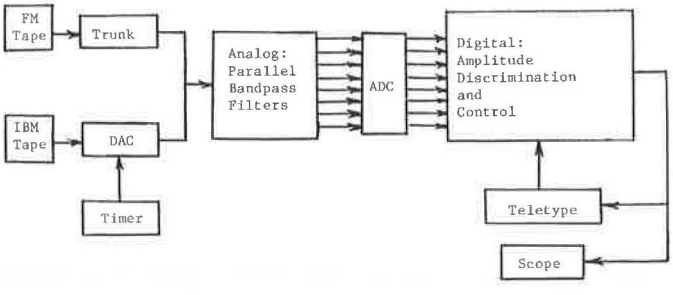

Table 4. Listing for run 7.

Time (sec)	Acceleration Amplitude (g)	Absorbed Power (W)		Time (sec)	Acceleration Amplitude (g)	Absorbed Power (W)	
		Unadjusted	Normalized			Unadjusted	Normalized
14.03	0.03	0.047	0.0011	42.14	0.04	0.091	0.0021
28.84	0.04	0.109	0.0026	45.00	0.06	0.228	0.0054
31.41	0.05	0.128	0.0030	81.91	0.03	0.047	0.0011
35.78	0.04	0.083	0.0020	96.03	0.03	0.047	0.0011

Table 5. Amplitude frequency output and absorbed power amplitude frequency distribution for run 7.

Item	Values							
Unadjusted AFD	0	0	0	0	0	0	0	0
	0	0	0	0	0	0	0	0
	0	1	0	0	0	0	0	1
	2	0	0	0	0	0	1	7
	0	0	1	1	6	1	5	28
	0	1	0	2	4	4	10	49
Normalized APAFD[a]	0.000	0.000	0.000	0.000	0.000	0.000	0.000	0.000
	0.000	0.000	0.000	0.000	0.000	0.000	0.000	0.000
	0.000	0.002	0.000	0.000	0.000	0.000	0.000	0.003
	0.001	0.000	0.000	0.000	0.000	0.000	0.010	0.009
	0.000	0.000	0.001	0.001	0.017	0.007	0.021	0.014
	0.000	0.000	0.000	0.001	0.005	0.011	0.017	0.010

[a]Sum = 0.130.

Figure 2. Absorbed power versus subjective rating for bus data.

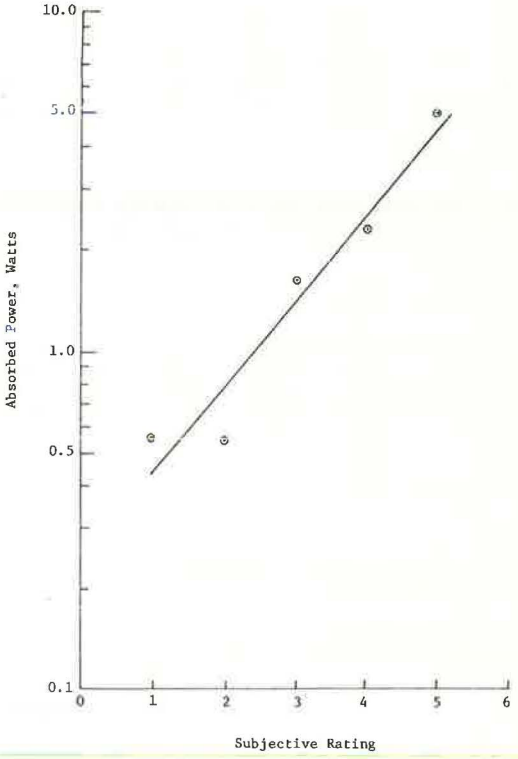

After the eight listings, the AFD is printed out and shows the number of peaks that occurred in each segment having a particular amplitude and frequency combination. A separate AFD is provided for each degree of freedom of each segment. Table 5 gives the AFD output for run 7, segment 3, vertical motion. This is a typical AFD, showing the approximate distribution found in most of the runs. In Table 5 the acceleration amplitude levels and frequency levels are set as follows:

Acceleration Amplitude (g)	Frequency (Hz)
0.03	0.06
0.05	0.12
0.08	0.25
0.13	0.50
0.21	1.00
0.32	2.00
0.50	4.00
	8.00
	16.00

The unadjusted APAFD and normalized APAFD are then printed out. These give the unadjusted AP and normalized AP contributed by each amplitude-frequency combination. The unadjusted APAFDs are not shown since they have no meaning; the normalized APAFD output is given in Table 5 for run 7, segment 3, vertical motion. The total unadjusted APAFB and the total normalized APAFD of the segment are printed out as a single number found by summing their respective values.

Subjective Ride Data

The subjective bus ride data used in the correlation studies were taken by experimenters of Old Dominion University and supplied by NASA. For runs 2 and 6, the subject assigned a number from 1 to 5 to the quality of the ride, where 1 was the best quality ride and 5 was the worst. Runs 7 and 8 were similar, except that the scale ranged from 1 to 6. The subjective data for runs 1, 3, 4, and 5 were unusable; therefore, the objective data for these runs were not processed. The objective and subjective data were tabulated for the correlation studies.

In a given run, all the AP values corresponding to a single subjective response number were averaged, and then standard deviation from this average was calculated. It was noted that a few extremely large acceleration values, especially in the lateral and longitudinal degrees of freedom, were causing large AP values where the subjective rating was small. These AP values were discarded because such accelerations were large enough to move the passengers from their seats and were unreasonable since the subjective responses were small.

A final composite correlation plot, combining the data for all segments of all runs from both accelerometers, was made. Although, in the individual plots, the curve was not always exponential as expected, the composite plot of all the data shown in Figure 2 is an exponential curve and fits the following equation:

$$S = 1.7245 \ln (3.96849\ AP) \tag{2}$$

where

S = subjective response and
AP = absorbed power in watts.

Appraisal of Results and Applications

The correlation results of AP as an objective ride measure to the subjective evaluation for the NASA bus data were successful. Individual segments and rides gave poor correlation since the data base was too small to give a reasonable random sample. How-

ever, when sufficient numbers of rides were used to give a reasonable sample base, excellent correlation was obtained, and the following logarithmical relation was shown by the data:

$$S = 1.7245 \ln (3.96849\ AP) \quad (3)$$

where

S = subjective rating (on a five-point scale) and
AP = absorbed power in watts.

Since there was a successful correlation of the bus data, a further correlation of International Standardization Organization (ISO) standards and the AP method was started (10). These two methods were found to agree rather well. In the whole-body frequency range, AP is slightly more conservative; in the 10 to 100-Hz range, the two agree; but, in the range equal to or lower than 2 Hz, AP is not so restrictive as ISO standards. Since AP only accounts for vibration effects and such things as motion sickness are not included, there is justification for the harsher requirements of ISO standards in this range. Since the two methods compare reasonably well, one can use either method as an overall criterion. However, the AP method has the distinct advantage that effects due to more than 1 degree of freedom can be determined by adding the effect of the individual degrees of freedom. It thus appears that, if the proposed ISO standards are to be used, a combination of ISO standards and the AP method would be in order.

When the bus-subjective and ISO standard correlations with AP have been made, it is useful to compare these two correlations. The following table gives the AP values (W) for both correlations (the ISO standards for 1-hour exposure).

Subjective Ratings	ISO Standards (avg)	Bus Ride
1	0.15	0.45
2	—	0.80
3	1.50	1.44
4	—	2.56
5	5.88	4.57

With the exception of the very good ride, the two correlations give AP levels that are very similar. Even the very good ride (subjective rating of 1) is close in terms of overall rating: range of 0.45 to 4.57 AP for the bus data and of 0.15 to 5.88 AP for the ISO standards.

CONCLUSIONS

This study has shown that the AP criterion of comfort measurement does indeed correlate well with subjective passenger response based on 3 degrees of freedom. Additiona research should be undertaken to correlate objective with subjective ride measures for other types of transportation systems and for additional degrees of freedom.

REFERENCES

1. A. D. Brickman, J. C. Wambold, and J. R. Zimmerman. An Amplitude-Frequency Description of Road Roughness. HRB Special Rept. 116, 1971, pp. 53-67.

2. J. C. Wambold and J. R. Zimmerman. Hybrid Programs for Calculating the Joint Probability of Amplitude and Frequency of a Random Signal. Trans., Analog/Hybrid Computer Education Society, West Long Branch, N. J., Vol. 3, No. 7, July 1971, pp. 133-144.
3. J. C. Wambold and W. H. Park. A Data Processing Method Giving a Better Physical Description of Random Signals. Proc., 20th International Instrumentation Symposium, 1974, pp. 371-375; Instrumentation Technology, Vol. 21, No. 6, June 1974, pp. 36-40.
4. F. Pradko and R. A. Lee. Vibration Comfort Criteria. Society of Automotive Engineers, Publ. 660139, 1966.
5. F. Pradko and R. A. Lee. Analytical Analysis of Human Vibration. Society of Automotive Engineers, Publ. 680091, 1968.
6. F. Pradko, R. A. Lee, and V. Kauluz. Theory of Human Vibration Response. American Society of Mechanical Engineers, Publ. 66-WA/BHF-15, 1966.
7. A. D. Brickman, W. H. Park, and J. C. Wambold. Road Roughness Effects on Vehicle Performance. Pennsylvania Transportation and Traffic Safety Center, Pennsylvania State Univ., Rept. TTSC 7207, 1972.
8. J. C. Wambold, W. H. Park, and R. G. Vashlishan. A New Random Data Description and Its Use in Transferring Road Roughness to Vehicle Response. American Society of Mechanical Engineers, Paper 73-DET-26, Sept. 1973.
9. W. H. Park, J. C. Wambold, and R. G. Vashlishan. Prediction of Objective Passenger Comfort From Road Profile. American Society of Mechanical Engineers, Paper 73-DET-114, Sept. 1973.
10. J. C. Wambold and W. H. Park. Objective Ride Quality Evaluation. Pennsylvania Transportation Institute, Pennsylvania State Univ., Rept. PTI 7412, March 1974.

SPONSORSHIP OF THIS RECORD

GROUP 2—DESIGN AND CONSTRUCTION OF TRANSPORTATION FACILITIES
W. B. Drake, Kentucky Department of Transportation, chairman

PAVEMENT DESIGN SECTION
Carl L. Monismith, University of California, Berkeley, chairman

Committee on Surface Properties-Vehicle Interaction
W. E. Meyer, Pennsylvania State University, chairman
Glenn G. Balmer, Frederick E. Behn, Andrius A. Butkunas, A. Y. Casanova III, Michael W. Fitzpatrick, William Gartner, Jr., Ralph C. G. Haas, Douglas I. Hanson, Don L. Ivey, William F. Lins, David C. Mahone, Paul Milliman, Alexander B. Moore, E. W. Myers, Arthur H. Neill, Jr., Bayard E. Quinn, John J. Quinn, Frederick A. Renninger, Rolands L. Rizenbergs, Hollis B. Rushing, Richard K. Shaffer, George B. Sherman, Elson B. Spangler, James C. Wambold, M. Lee Webster, E. A. Whitehurst, Ross G. Wilcox, Dillard D. Woodson

Lawrence F. Spaine, Transportation Research Board staff

The organizational units and the chairmen and members are as of December 31, 1974.